

Sonogashira (Cu and amine free) and Suzuki coupling in air catalyzed *via* nanoparticles formed *in situ* from Pd(II) complexes of chalcogenated Schiff bases of 1-naphthaldehyde and their reduced forms

Renu Bhaskar, Alpesh K. Sharma, Manoj K. Yadav and Ajai K. Singh*

Department of Chemistry, Indian Institute of Technology Delhi, New Delhi-110016, India

Table of Contents:

Table S1-S2	Crystal Data and Structural Refinement Parameters of L1 , Complexes 1 , 2 , 3 and 4	3-5
Table S3-S4	Selected Bond Lengths and Bond Angles of L1 , Complexes 1 , 2 , 3 and 4	6-8
Table S5	Intermolecular Interactions in Complexes 1 , 2 , 3 and 4	8
Figure S1-S16	SEM-EDX and Size Distribution of NPs	9-15
Figure S17-S69	Mass and NMR data	16-43
Figure S70-S87	TGA, UV-Vis and FT-IR spectra of NPs	44-52
Figure S88-S91	Intermolecular interactions in 1-4	53-54

Two-Phase Test

A mixture of 4-bromobenzoic acid-immobilized silica (0.20 g) (prepared by reported methods)¹, phenylboronic acid (0.36 g, 3 mmol) (SMC)/ phenyl acetylene (2 mmol) (Sonogashira coupling), (0.224 g, 2.2 mmol), 4-bromoacetophenone (0.20 g, 1.0 mmol), and K₂CO₃ (0.441 g, 3.0 mmol) were heated in an inert atmosphere at 100 °C for 12 h in DMF + water (3:1) (4 mL) (SMC)/DMF (1 mL) (Sonogashira coupling) in the presence of 2 mol% of **1**. After completion of the reaction, the mixture was cooled and filtered through a G-4 crucible. The residue left in the crucible was washed with 20 mL of water followed by diethyl ether (2×20 mL). The filtrate and washings were collected together. The resulting mixture was

extracted with 30 mL of diethyl ether. The solvent of the extract was evaporated and the residue was analyzed with ^1H NMR. The yield of the cross-coupled product for both coupling reactions was ~95%. The residue in G-4 crucible was hydrolysed with KOH (1.68 g dissolved in 10 mL of EtOH + 5 mL of H₂O) at 90 °C for 3 days. The hydrolysed solution was neutralized with aqueous 20% (v/v) HCl and, extracted with dichloromethane (30 mL) followed by ethyl acetate (40 mL). The organic phases were combined together and its solvent was evaporated off. The hydrolyzed products were analyzed by ^1H NMR spectroscopy.

General Procedure for the Catalytic Life of 1

In a round bottom flask, 4-bromobenzaldehyde (1.0 mmol), phenylboronic acid (1.3 mmol)(SMC)/phenyl acetylene (2 mmol) (Sonogashira coupling) and K₂CO₃ (2.0 mmol) (SMC) / (1.3 mmol) (Sonogashira coupling) and catalyst **1** (0.01 mol % (SMC)/ 0.05 mol % (Sonogashira coupling) in DMF + water (3:1) (4 mL) (SMC)/DMF (1 mL) (Sonogashira coupling) were heated at 90 °C for 1 h (Sonogashira coupling) /2 h (SMC). The reaction mixture was stirred at 80 °C. After 1/2 hours, the mixture was cooled to the ambient temperature. An aliquot (100 μL) was taken for analysis by ^1H NMR spectroscopy, and a new batch of 4-bromobenzaldehyde (1.0 mmol), base (2.0 mmol) (SMC) / (1.3 mmol) (Sonogashira coupling), phenylboronic acid (1.3 mmol) (SMC)/phenyl acetylene (2 mmol) (Sonogashira coupling) was directly added. The reaction mixture was stirred at 80 °C for another 1/2 hours. Aliquot analysis by ^1H NMR and substrate addition was repeated for eight times.

Table S1 Crystal Data and Structural Refinement Parameters of Complexes 1-4.

Compounds	1	2	3	4
Empirical formula	C ₁₉ H ₁₆ ClNPdS	C ₁₉ H ₁₆ ClNPdSe	C ₃₉ H ₄₀ Cl ₆ N ₂ Pd ₂ S ₂	C ₂₀ H ₂₀ Cl ₅ NPdSe
Formula wt.	432.24	479.14	1026.35	636.98
Crystal size [mm]	0.28×0.27×0.2	0.30×0.28×0.26	0.29×0.28×0.26	0.28×0.27×0.26
Crystal system	Monoclinic	Orthorhombic	Triclinic	Monoclinic
Space group	<i>P</i> 2 <i>1/n</i>	<i>P</i> 2 <i>1</i> 2 <i>1</i> 2 <i>1</i>	<i>P</i> - <i>I</i>	<i>P</i> 2 <i>1/n</i>
Unit Cell dimensions	a = 14.971(2) Å b = 8.5731(12) Å c = 26.443(4) Å α = 90.00° β = 96.075(2)° γ = 90.00°	a = 5.5753(19) Å b = 8.462(3) Å c = 36.235(12) Å α = 90° β = 90° γ = 90°	a = 9.2268(17) Å b = 11.055(2) Å c = 21.199(4) Å α = 84.460° β = 82.473(4)° γ = 72.438(4)°	a = 15.624(2) Å b = 9.9535(14) Å c = 15.700(2) Å α = 90° β = 94.120(3)° γ = 90°
Volume [Å ³]	3374.8(8)	1709.5(10)	2040.1(7)	2435.3(6)
Z	8	4	2	4
Density (Calc.) [Mg·m ⁻³]	1.701	1.862	1.671	1.737
Absorption coeff. [mm ⁻¹]	1.379	3.368	1.408	2.812
<i>F</i> (000)	1728.0	936.0	1028.0	1248.0
θ range [°]	1.549–24.998	2.248–24.997	0.971–24.999	1.909–24.994
Index ranges	-17≤ <i>h</i> ≤ 17	-6≤ <i>h</i> ≤ 6	-10≤ <i>h</i> ≤ 9	-18≤ <i>h</i> ≤ 18

	$-10 \leq k \leq 10$ $-31 \leq l \leq 31$	$-10 \leq k \leq 10$ $-43 \leq l \leq 43$	$-13 \leq k \leq 13$ $-25 \leq l \leq 21$	$-11 \leq k \leq 11$ $-18 \leq l \leq 18$
Reflections collected	31550	16432	10511	22813
Independent reflections ($R_{\text{int.}}$)	5934 (0.0436)	3005 (0.0445)	7072 (.0495)	4260(0.0699)
Max./min. Transmission	0.699/0.685	0.418/0.378	0.694/0.670	0.482/0.472
Data/restraints/parameters	5934/0/415	3005/0/209	7072/2/468	4260/1/257
Goodness-of-fit on F^2	1.234	1.146	0.994	1.011
Final R indices [$I > 2\sigma(I)$]	$R_I = 0.0445$ $wR_2 = 0.0995$	$R_I = 0.0393$ $wR_2 = 0.0937$	$R_I = 0.0736$ $wR_2 = 0.1361$	$R_I = 0.0584$ $wR_2 = 0.1485$
R indices (all data)	$R_I = 0.0503$, $wR_2 = 0.1022$	$R_I = 0.0410$ $wR_2 = 0.0946$	$R_I = 0.1330$ $wR_2 = 0.1598$	$R_I = 0.0961$ $wR_2 = 0.1690$
Largest diff. peak/hole [e. \AA^3]	0.493/-0.699	0.646/-0.698	0.819/-0.683	0.809/-0.651

Table S2 Crystal Data and Structural Refinement Parameters of Ligand L1

Compounds	L1
Empirical formula	C19 H17 N S
Formula wt.	291.40
Crystal size [mm]	0.29×0.27×0.26
Crystal system	Monoclinic
Space group	<i>P</i> 21
Unit Cell dimension	$a = 5.274(2)\text{\AA}$ $b = 14.195(6)\text{\AA}$ $c = 10.646(4)\text{\AA}$ $\alpha = 90.00^\circ$ $\beta = 101.610(8)^\circ$ $\gamma = 90.00^\circ$
Volume [\AA^3]	776.7(5)
<i>Z</i>	2
Density (Calc.) [$\text{Mg}\cdot\text{m}^{-3}$]	1.246
Absorption coeff. [mm^{-1}]	0.201
<i>F</i> (000)	308.0
θ range [$^\circ$]	1.953–24.999
Index ranges	$-6 \leq h \leq 6$ $-16 \leq k \leq 16$ $-9 \leq l \leq 12$
Reflections collected	3946
Independent reflections ($R_{\text{int.}}$)	2617 (0.0271)
Max./min. Transmission	0.950/0.942
Data/restraints/parameters	2617/1/190
Goodness-of-fit on F^2	1.034
Final R indices [$I > 2\sigma(I)$]	$R_I = 0.0617$ $wR_2 = 0.1343$
R indices (all data)	$R_I = 0.0777,$ $wR_2 = 0.1438$
Largest diff. peak/hole [$e\cdot\text{\AA}^{-3}$]	0.472/–0.166

Table S3 Selected Bond Lengths and Bond Angles of L1

Bond Length (Å)		Bond Angle (°)	
S(1)-C(6)	1.765(6)	C(6)-S(1)-C(7)	104.8(3)
S(1)-C(7)	1.800(7)	C(5)-C(6)-S(1)	124.7(5)
N(1)-C(9)	1.141(8)	C(1)-C(6)-S(1)	116.4(5)
N(1)-C(8)	1.471(9)	C(8)-C(7)-S(1)	110.1(4)
C(1)-C(6)	1.381(8)	C(9)-N(1)-C(8)	120.2(8)
		N(1)-C(8)-C(7)	110.2(5)
		N(1)-C(9)-C(10)	125.5(8)
		C(6)-C(1)-C(2)	120.5(7)

Table S4 Selected Bond Lengths and Bond Angles of 1-4

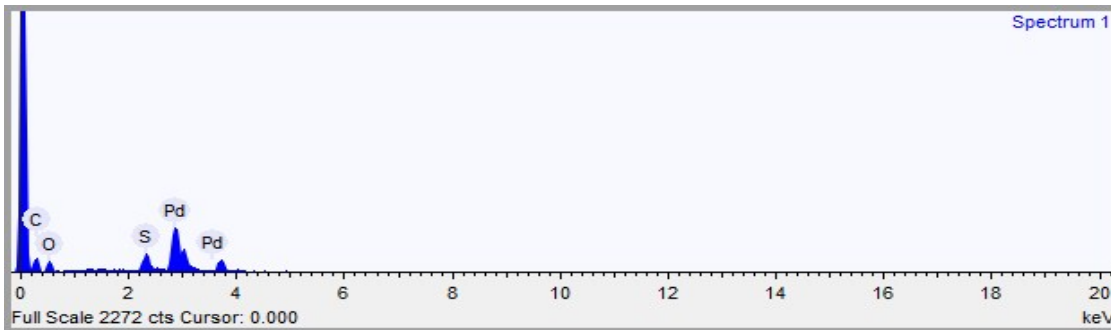
Complex	Bond Length [Å]		Bond Angle [°]	
1	Pd(1)-N(1)	1.994(4)	N(1)-Pd(1)-C(12)	91.41(17)
	Pd(1)-C(12)	2.009(4)	N(1)-Pd(1)-Cl(1)	173.05(11)
	Pd(1)-Cl(1)	2.332(13)	C(12)-Pd(1)-Cl(1)	95.22(13)
	Pd(1)-S(1)	2.426(12)	N(1)-Pd(1)-S(1)	86.05(11)
	S(1)-C(6)	1.785(5)	C(12)-Pd(1)-S(1)	174.60(13)
	S(1)-C(7)	1.815(5)	Cl(1)-Pd(1)-S(1)	87.17(4)
	N(1)-C(9)	1.269(6)	C(6)-S(1)-C(7)	102.0(2)
	N(1)-C(8)	1.479(6)	C(6)-S(1)-Pd(1)	108.94(16)
	C(8)-C(7)	1.504(7)	C(7)-S(1)-Pd(1)	94.88(17)
	C(1)-C(6)	1.376(7)	C(13)-C(12)-Pd(1)	119.4(4)
	C(10)-C(9)	1.452(7)	C(11)-C(12)-Pd(1)	122.9(3)
			C(19)-C(10)-C(9)	116.3(5)
			C(11)-C(10)-C(9)	122.7(4)
			C(9)-N(1)-C(8)	117.8(4)
			C(9)-N(1)-Pd(1)	127.7(3)
			C(8)-N(1)-Pd(1)	114.3(3)
			C(1)-C(6)-S(1)	120.3(4)
			C(5)-C(6)-S(1)	119.3(4)
			N(1)-C(9)-C(10)	126.6(4)
			N(1)-C(8)-C(7)	111.1(4)
			C(8)-C(7)-S(1)	110.4(3)
2	C(1)-C(6)	1.378(11)	N(1)-Pd(1)-C(12)	91.8(3)
	Pd(1)-N(1)	1.981(6)	N(1)-Pd(1)-Cl(1)	172.0(2)
	Pd(1)-C(12)	2.026(8)	C(12)-Pd(1)-Cl(1)	96.3(3)
	Pd(1)-Cl(1)	2.341(2)	N(1)-Pd(1)-Se(1)	86.6(2)

	Pd(1)-Se(1)	2.523(11)	C(12)-Pd(1)-Se(1)	178.1(2)
	Se(1)-C(6)	1.933(8)	Cl(1)-Pd(1)-Se(1)	85.40(7)
	Se(1)-C(7)	1.940(8)	C(6)-Se(1)-C(7)	98.5(4)
	C(9)-C(10)	1.462(12)	C(6)-Se(1)-Pd(1)	102.0(2)
	N(1)-C(9)	1.278(10)	C(7)-Se(1)-Pd(1)	91.3(3)
	N(1)-C(8)	1.498(10)	C(13)-C(12)-Pd(1)	119.3(7)
	C(7)-C(8)	1.480(12)	C(11)-C(12)-Pd(1)	124.0(6)
			C(19)-C(10)-C(9)	115.2(9)
			C(11)-C(10)-C(9)	122.0(7)
			C(9)-N(1)-C(8)	115.5(7)
			C(9)-N(1)-Pd(1)	127.7(6)
			C(8)-N(1)-Pd(1)	116.9(5)
			C(1)-C(6)-Se(1)	121.6(7)
			C(5)-C(6)-Se(1)	118.2(6)
			N(1)-C(9)-C(10)	127.4(8)
			C(7)-C(8)-N(1)	112.1(7)
			C(8)-C(7)-Se(1)	110.2(7)
3	C(1)-C(6)	1.365(12)	N(1)-Pd(1)-S(1)	87.7(2)
	Pd(1)-N(1)	2.084(7)	N(1)-Pd(1)-Cl(1)	92.5(2)
	Pd(1)-Cl(1)	2.311(2)	N(1)-Pd(1)-Cl(2)	175.9(2)
	Pd(1)-Cl(2)	2.301(2)	S(1)-Pd(1)-Cl(1)	179.49(10)
	Pd(1)-S(1)	2.259(2)	S(1)-Pd(1)-Cl(2)	88.59(9)
	S(1)-C(6)	1.778(8)	Cl(2)-Pd(1)-Cl(1)	91.19(9)
	S(1)-C(7)	1.809(9)	C(6)-S(1)-C(7)	101.3(4)
	C(9)-C(10)	1.521(12)	C(6)-S(1)-Pd(1)	106.5(3)
	N(1)-C(8)	1.497(11)	C(7)-S(1)-Pd(1)	96.9(3)
	N(1)-C(9)	1.498(11)	C(8)-N(1)-C(9)	110.7(7)
	C(7)-C(8)	1.498(13)	C(8)-N(1)-Pd(1)	112.5(6)
			C(9)-N(1)-Pd(1)	116.2(6)
			N(1)-C(9)-C(10)	113.1(8)

4	C(1)-C(6)	1.367(11)	N(1)-Pd(1)-Se(1)	88.44(18)
	Pd(1)-N(1)	2.090(6)	N(1)-Pd(1)-Cl(1)	175.39(18)
	Pd(1)-Cl(1)	2.300(2)	N(1)-Pd(1)-Cl(2)	92.24(19)
	Pd(1)-Cl(2)	2.323(2)	Se(1)-Pd(1)-Cl(1)	87.63(6)
	Pd(1)-Se(1)	2.369(10)	Se(1)-Pd(1)-Cl(2)	178.26(6)
	Se(1)-C(6)	1.948(7)	Cl(2)-Pd(1)-Cl(1)	91.62(8)
	Se(1)-C(7)	1.951(7)	C(6)-Se(1)-C(7)	98.0(3)
	C(9)-C(10)	1.498(11)	C(6)-Se(1)-Pd(1)	104.2(2)
	N(1)-C(8)	1.487(10)	C(7)-Se(1)-Pd(1)	93.1(2)
	N(1)-C(9)	1.498(10)	C(8)-N(1)-C(9)	109.9(6)
	C(7)-C(8)	1.484(11)	C(8)-N(1)-Pd(1)	113.4(5)
	C(20)-Cl(4)	1.653(13)	C(9)-N(1)-Pd(1)	115.9(4)
	C(20)-Cl(3)	1.643(13)	N(1)-C(9)-C(10)	113.2(6)
	C(20)-Cl(5)	1.686(14)	C(1)-C(6)-Se(1)	116.8(7)
			C(5)-C(6)-Se(1)	122.6(6)
			C(8)-C(7)-Se(1)	109.6(5)
			N(1)-C(8)-C(7)	112.5(7)

Table S5 Non-covalent Interactions C–H···Cl Distances (Å) of 1-4

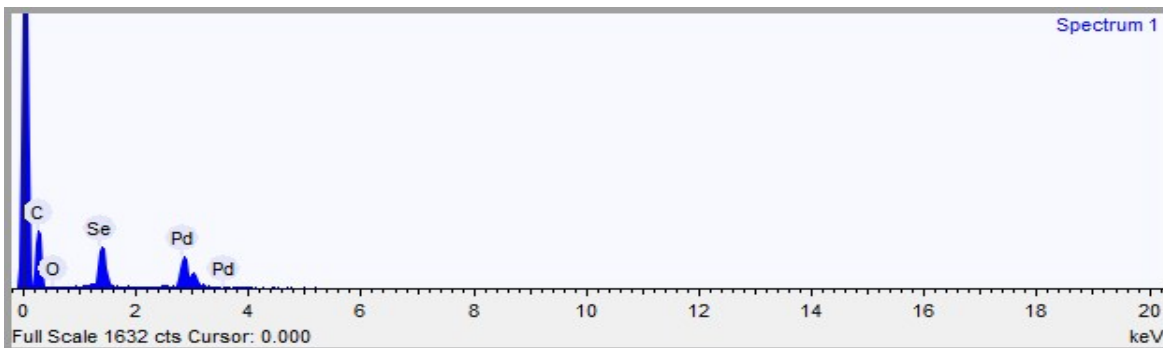
1	2	3	4
H9···Cl1 2.690	H9···Cl1 2.711	H34···Cl1 2.762	H17···Cl1 2.857
H23···Cl1 2.851		H7B···Cl2 2.844	H20···Cl1 2.859
		H39A···Cl2 2.554	H1A···Cl1 2.518
		H1A···Cl2 2.644	H7B···Cl2 2.895
		H26A···Cl3 2.919	
		H2A···Cl4 2.618	
		H18···Cl5 2.689	



Summary results

Element	Weight %	Weight % σ	Atomic %
Sulfur	9.985	0.627	26.906
Palladium	90.015	0.627	73.094

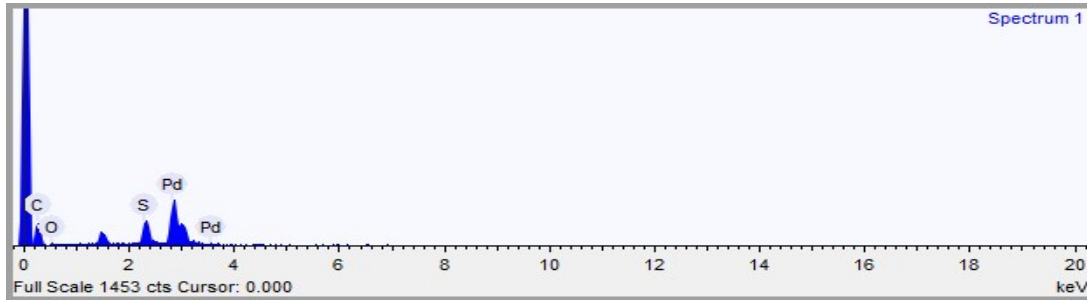
Fig. S1 SEM-EDX image of NPs obtained from **1** during Suzuki-Miyaura reaction



Summary results

Element	Weight %	Weight % σ	Atomic %
Selenium	39.880	1.536	47.198
Palladium	60.120	1.536	52.802

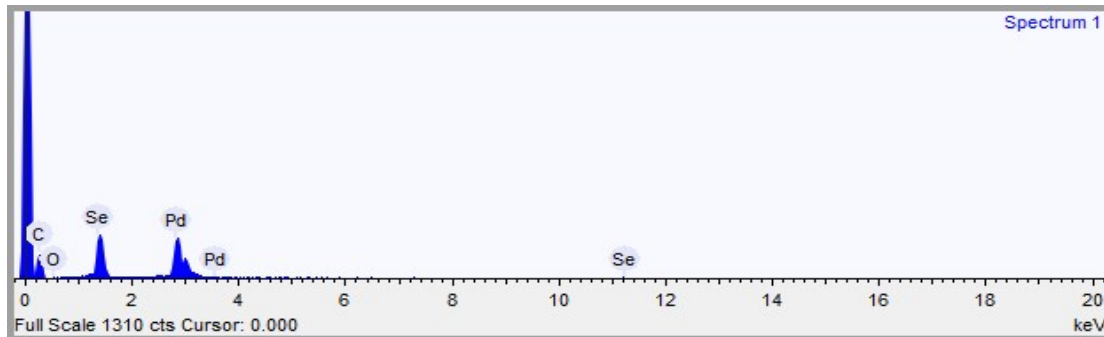
Fig. S2 SEM-EDX image of NPs obtained from **2** during Suzuki-Miyaura reaction



Summary results

Element	Weight %	Weight % σ	Atomic %
Sulfur	14.016	0.809	35.103
Palladium	85.984	0.809	64.897

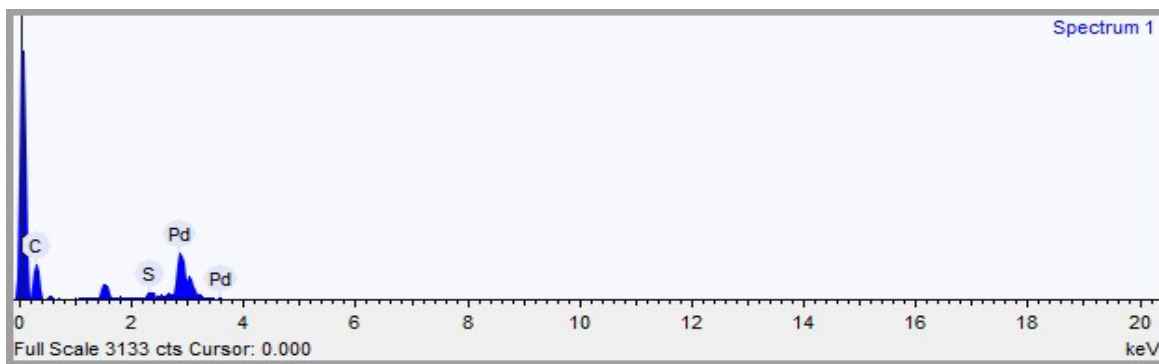
Fig. S3 SEM-EDX image of NPs obtained from **3** during Suzuki-Miyaura reaction



Summary results

Element	Weight %	Weight % σ	Atomic %
Selenium	35.833	1.501	42.939
Palladium	64.167	1.501	57.061

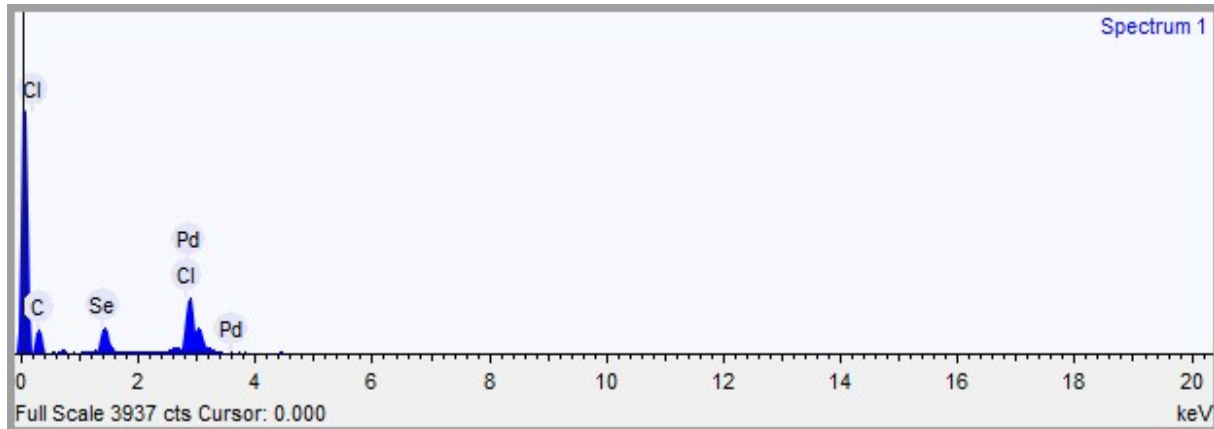
Fig. S4 SEM-EDX image of NPs obtained from **4** during Suzuki-Miyaura reaction



Summary results

Element	Weight %	Weight % σ	Atomic %
Sulfur	4.583	0.425	13.747
Palladium	95.417	0.425	86.253

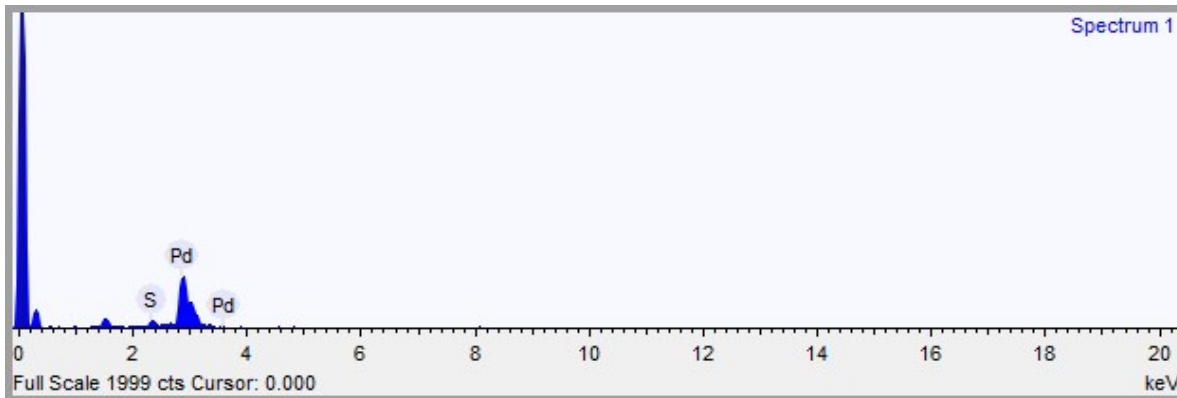
Fig. S5 SEM-EDX image of NPs obtained from **1** during Sonogashira coupling



Summary results

Element	Weight %	Weight % σ	Atomic %
Selenium	20.852	0.865	26.200
Palladium	79.148	0.865	73.800

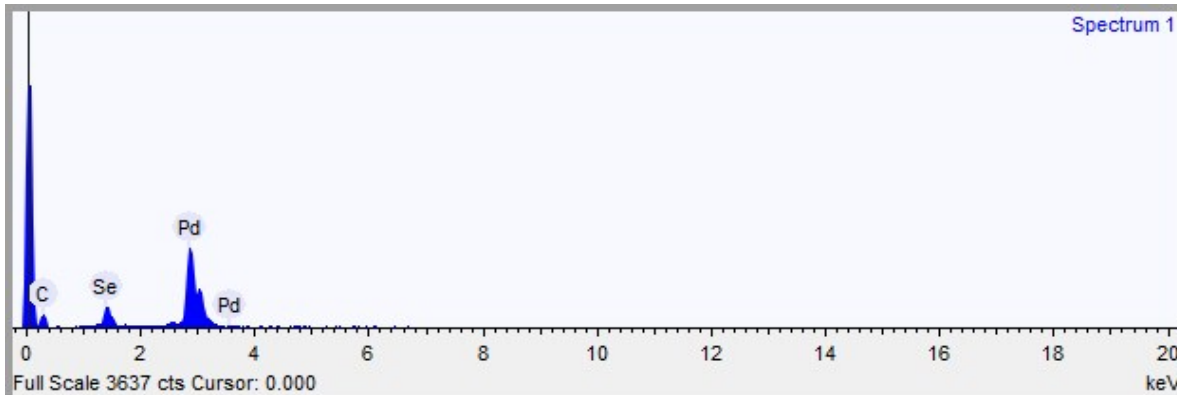
Fig. S6 SEM-EDX image of NPs obtained from **2** during Sonogashira coupling



Summary results

Element	Weight %	Weight % σ	Atomic %
Sulfur	4.272	0.494	12.898
Palladium	95.728	0.494	87.102

Fig. S7 SEM-EDX image of NPs obtained from 3 during Sonogashira coupling



Summary results

Element	Weight %	Weight % σ	Atomic %
Selenium	11.986	0.644	15.506
Palladium	88.014	0.644	84.494

Fig. S8 SEM-EDX image of NPs obtained from 4 during Sonogashira coupling

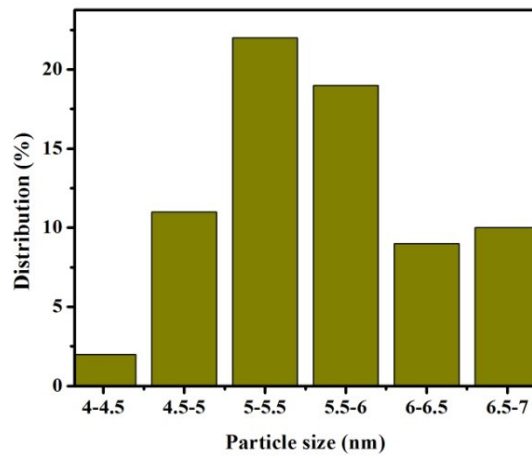


Fig. S9 Size-distribution curve of NPs isolated from **1** during Suzuki-Miyaura reaction

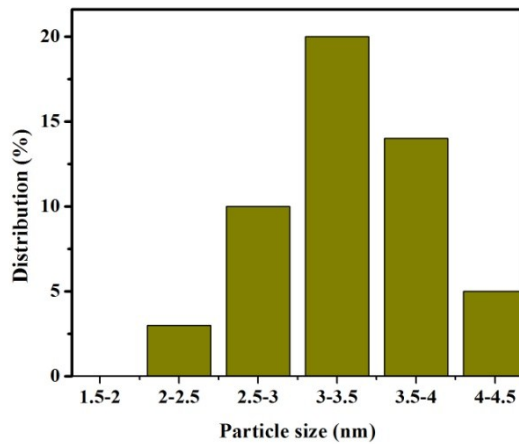


Fig. S10 Size-distribution curve of NPs isolated from **2** during Suzuki-Miyaura reaction

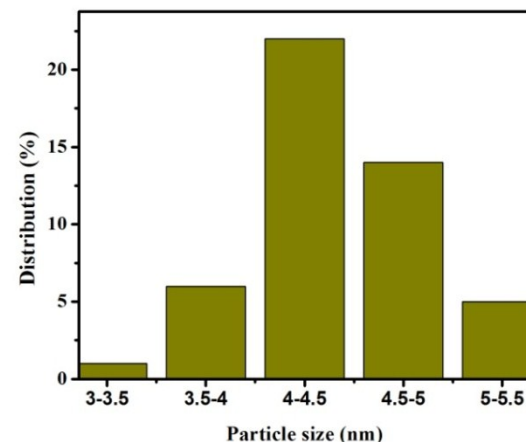


Fig. S11 Size-distribution curve of NPs isolated from **3** during Suzuki-Miyaura reaction

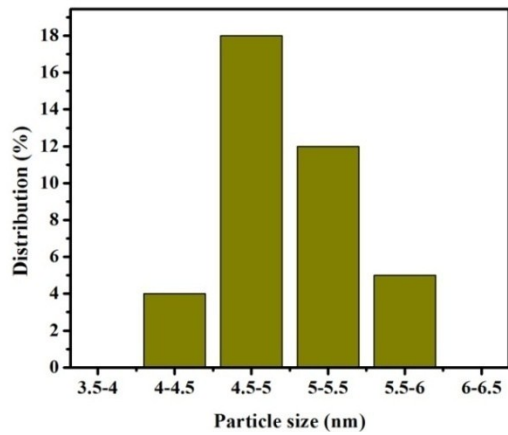


Fig. S12 Size-distribution curve of NPs isolated from **4** during Suzuki-Miyaura reaction

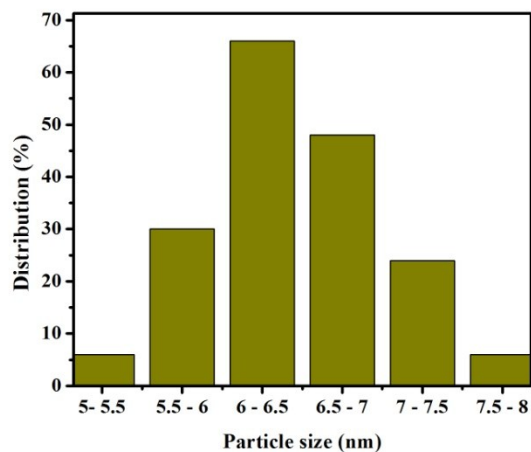


Fig. S13 Size-distribution curve of NPs isolated from **1** during Sonogashira coupling

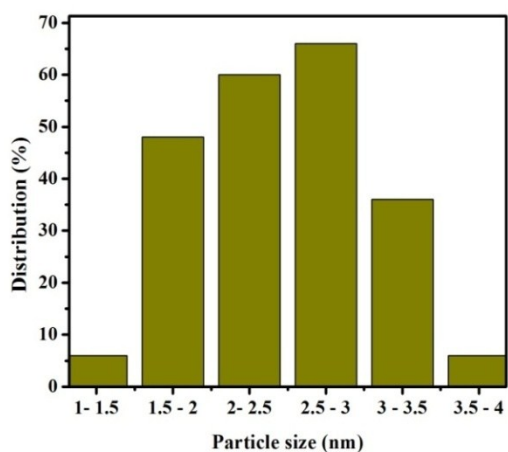


Fig. S14 Size-distribution curve of NPs isolated from **2** during Sonogashira coupling

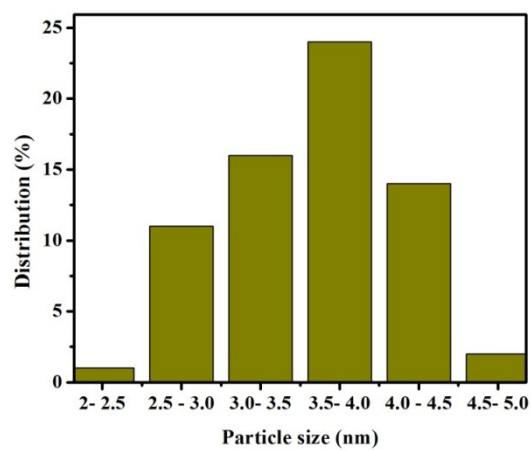


Fig. S15 Size-distribution curve of NPs isolated from **3** during Sonogashira coupling

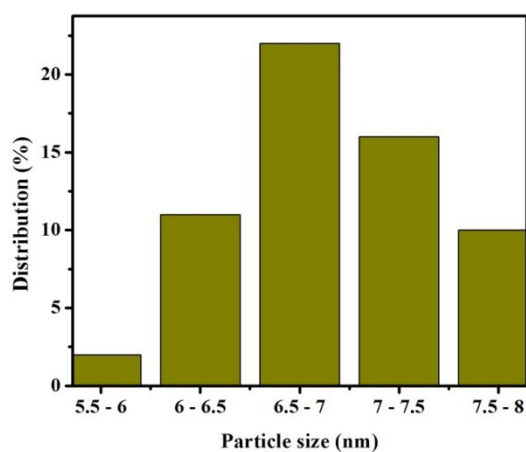


Fig. S16 Size-distribution curve of NPs isolated from **4** during Sonogashira coupling

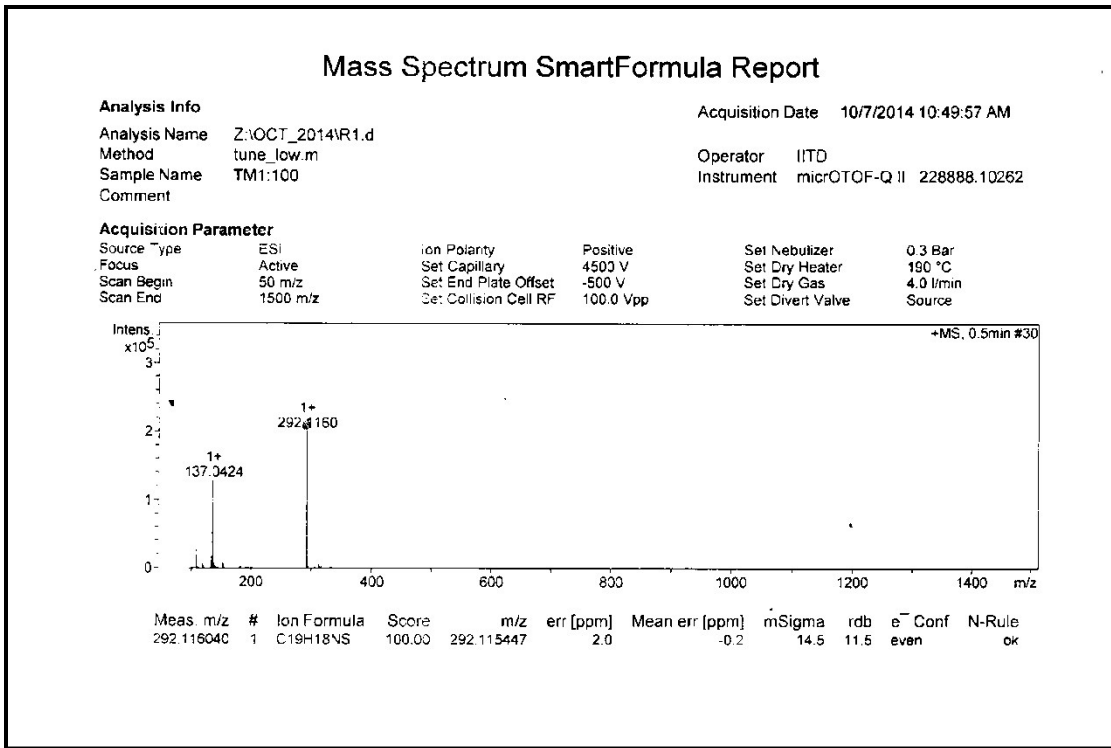


Fig. S17 Mass spectrum of L1

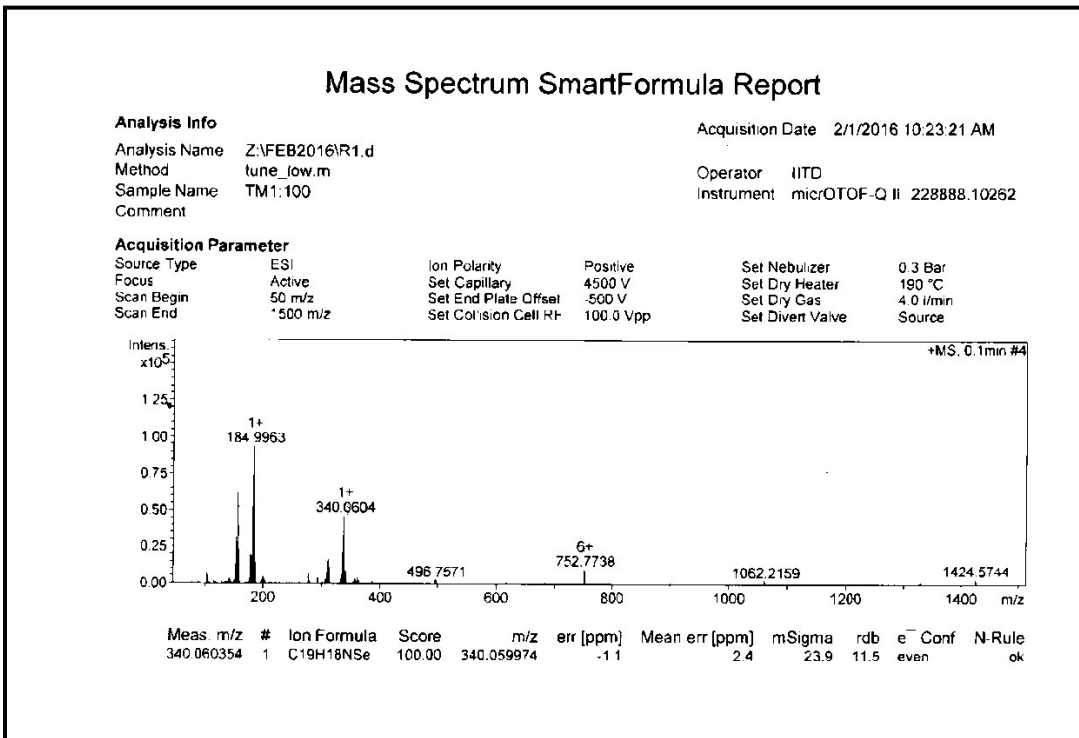


Fig. S18 Mass spectrum of L2

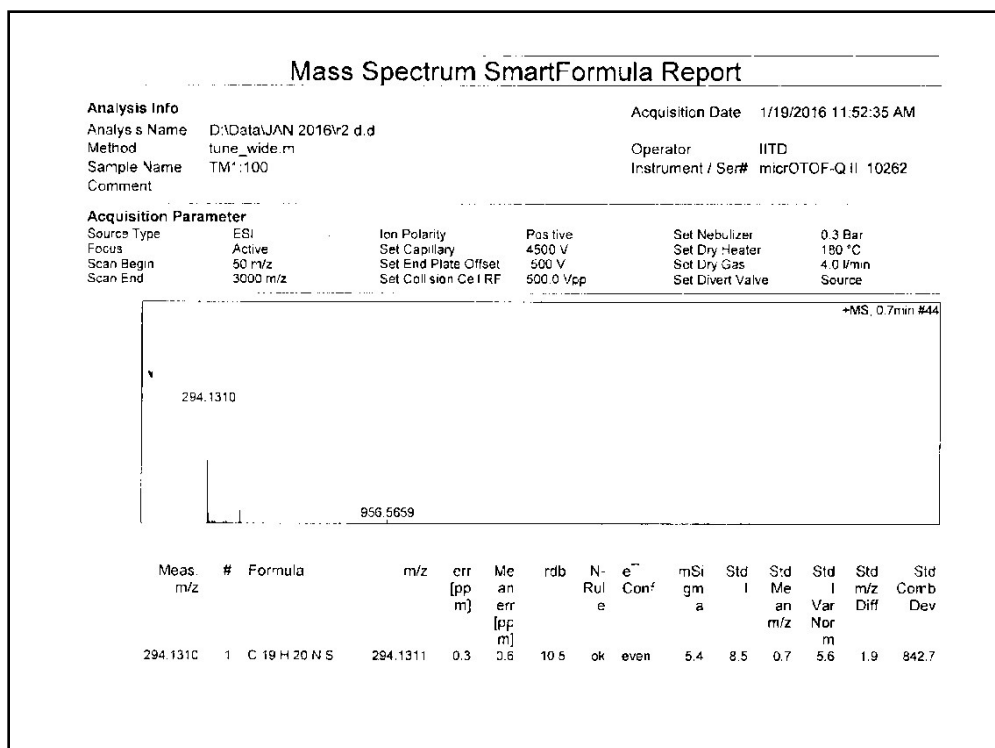


Fig. S19 Mass spectrum of L3

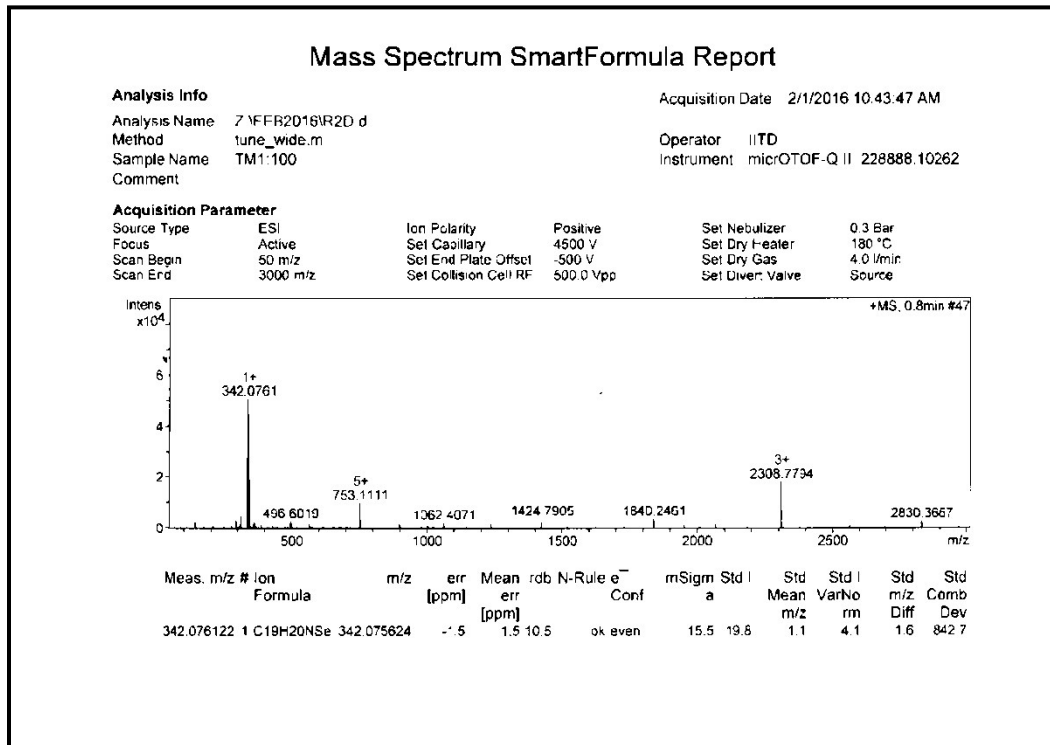


Fig. S20 Mass spectrum of L4

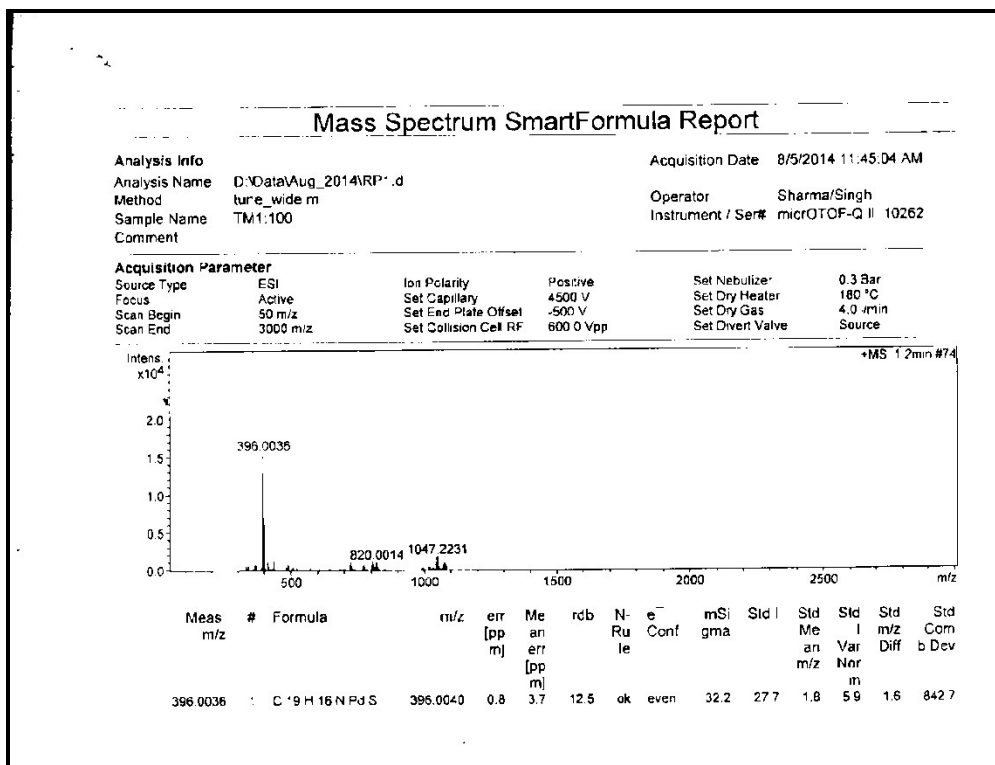


Fig. S21 Mass spectrum of complex 1

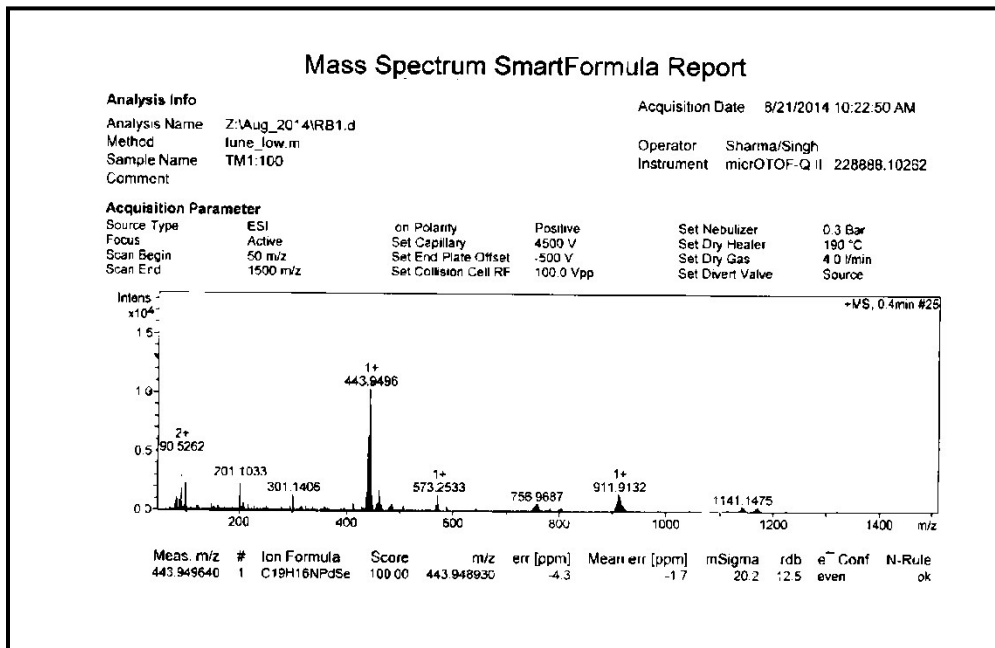


Fig. S22 Mass spectrum of complex 2

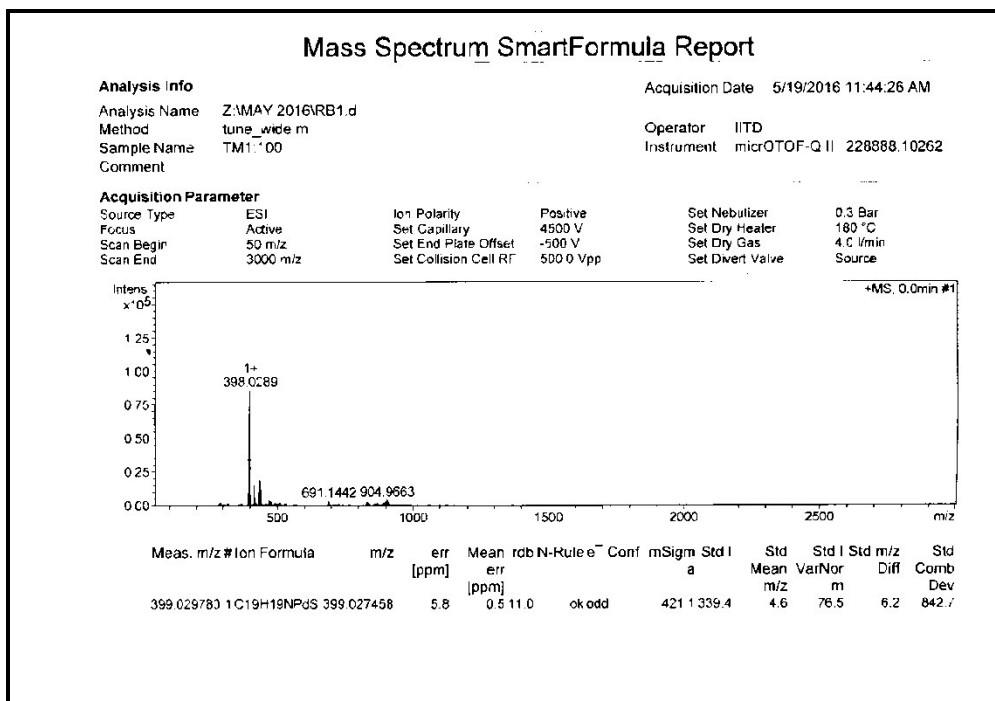


Fig. S23 Mass spectrum of complex 3

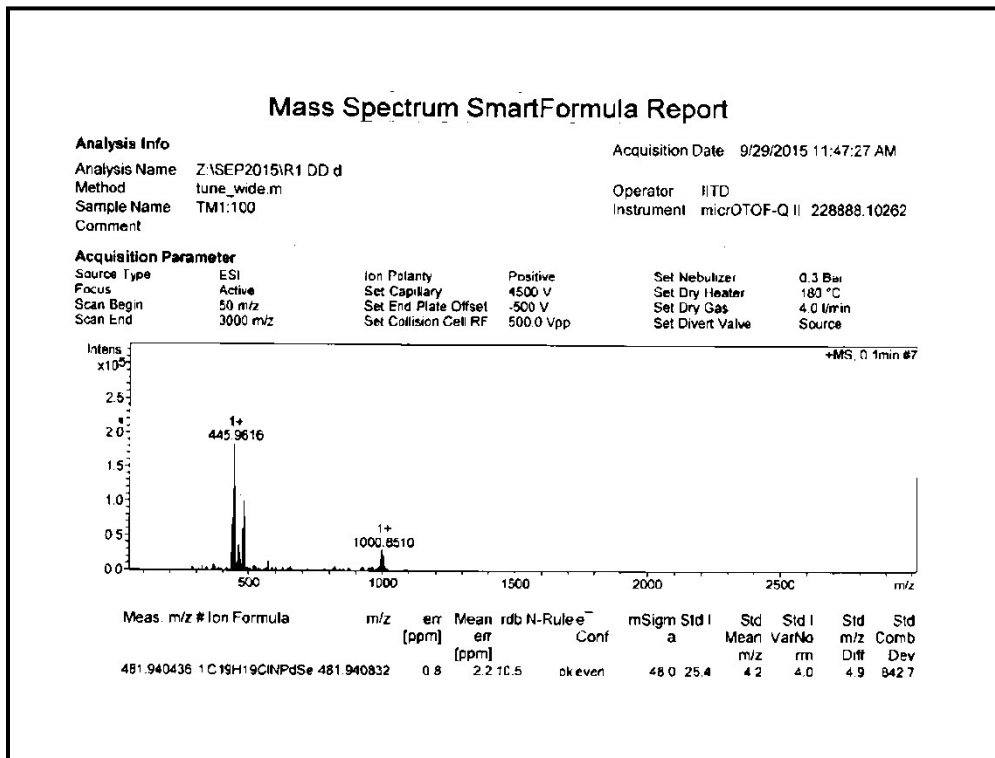


Fig. S24 Mass spectrum of complex 4

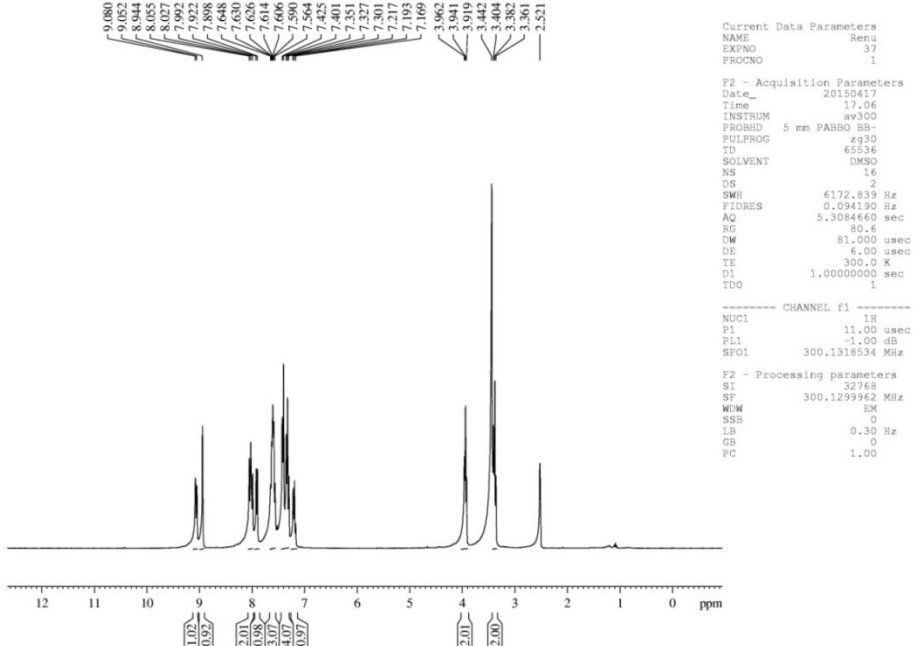


Fig. S25 ^1H NMR spectrum of ligand L1

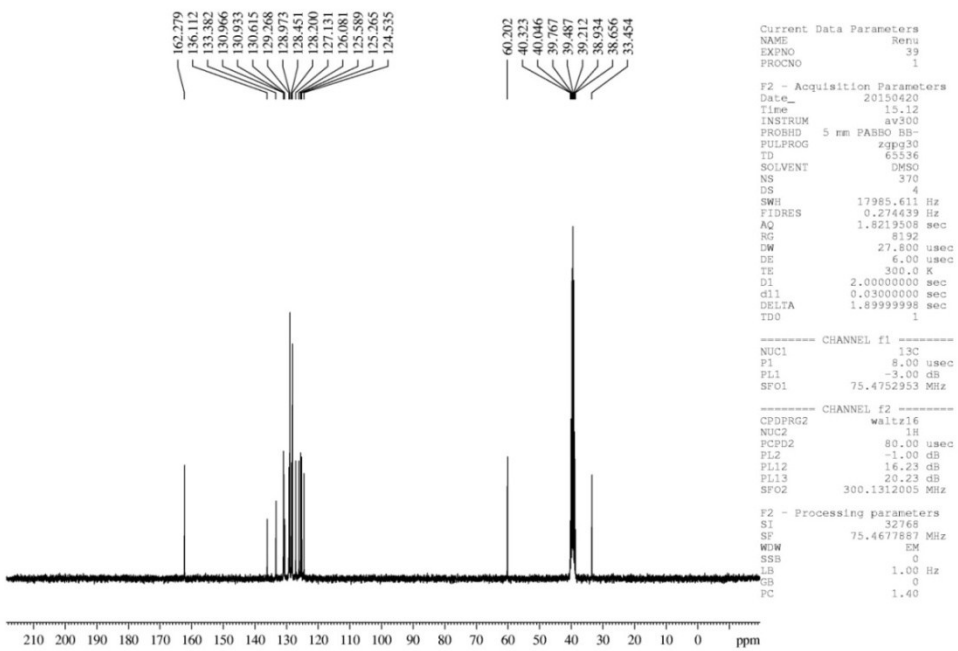


Fig. S26 $^{13}\text{C}\{^1\text{H}\}$ NMR spectrum of ligand L1

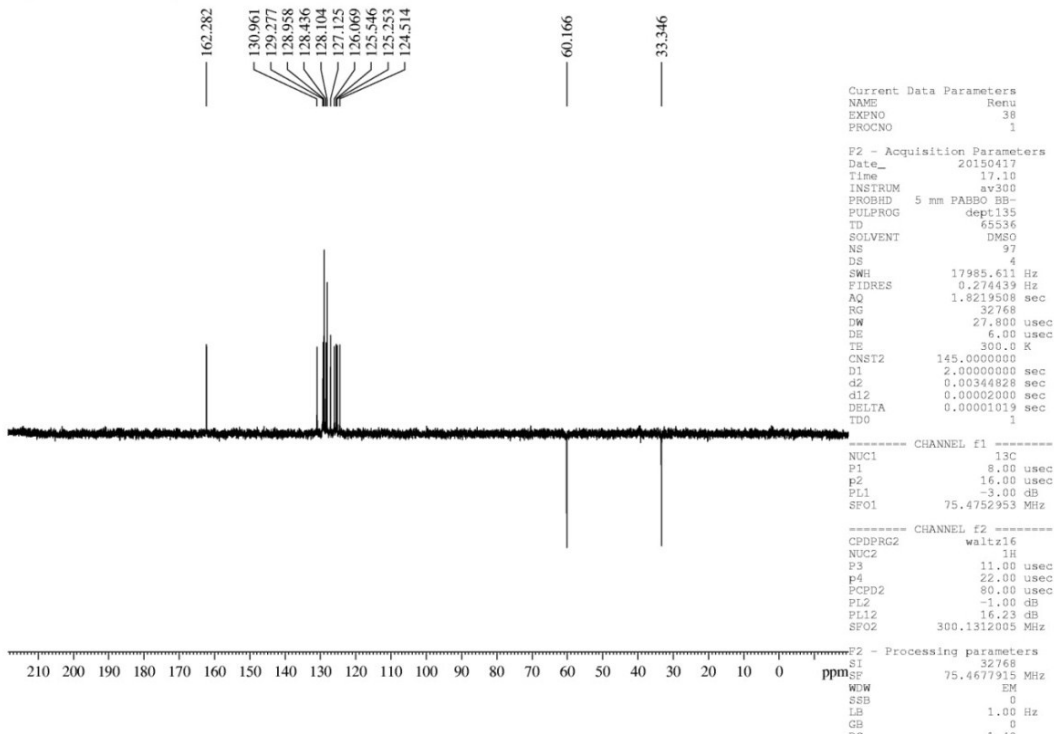


Fig. S27 $^{13}\text{C}\{\text{H}\}$ NMR-DEPT 135 spectrum of ligand L1

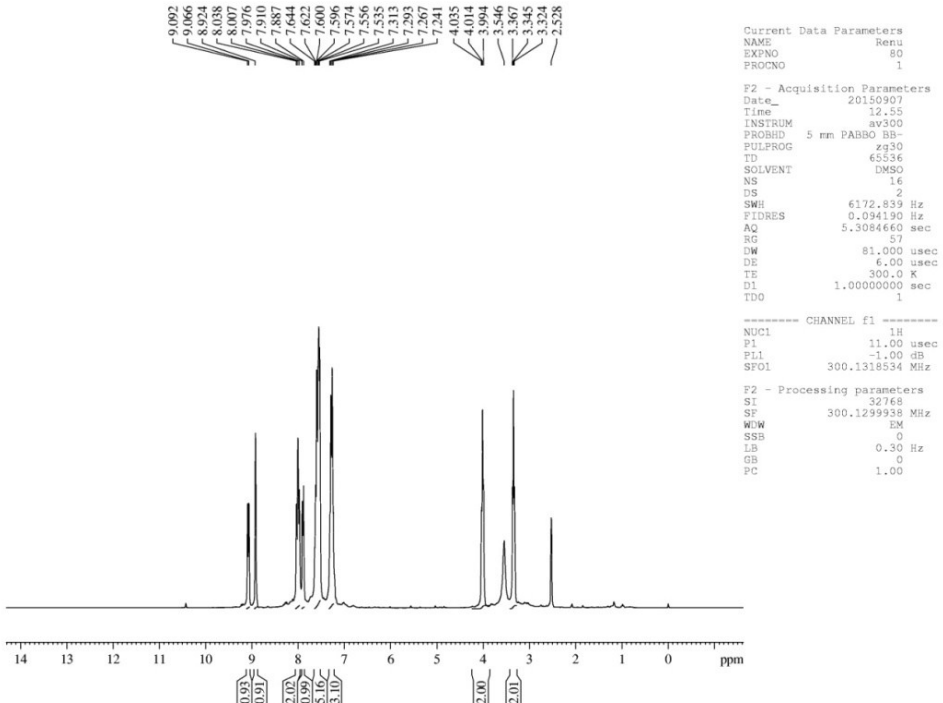


Fig. S28 ^1H NMR spectrum of ligand L2

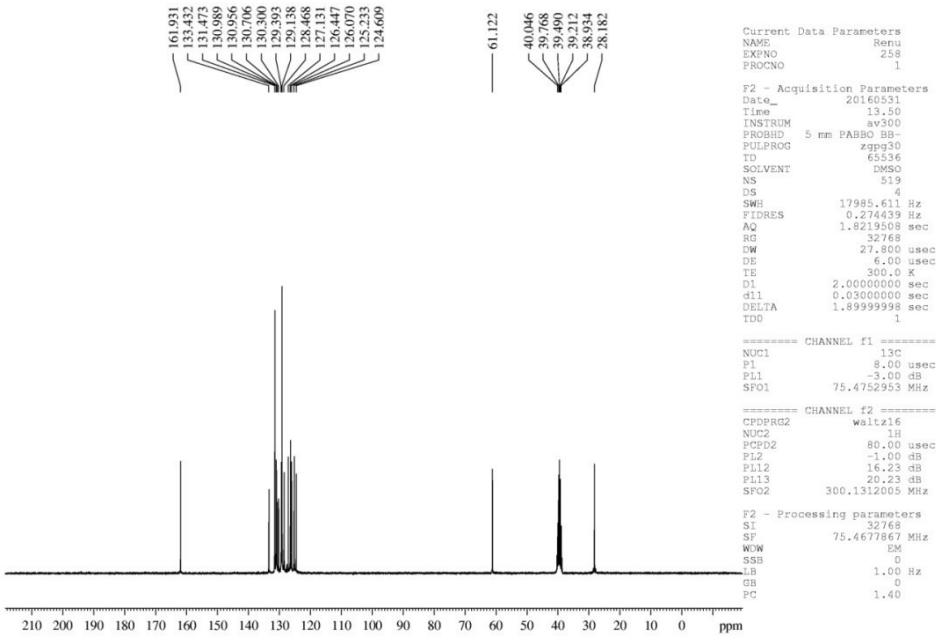


Fig. S29 $^{13}\text{C}\{\text{H}\}$ NMR spectrum of ligand **L2**

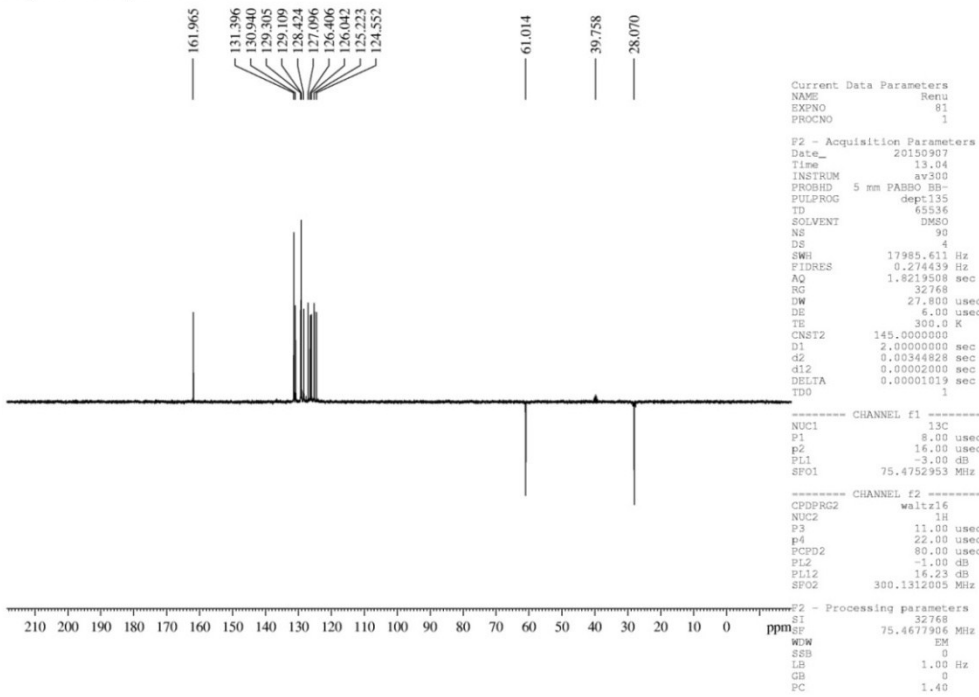


Fig. S30 $^{13}\text{C}\{\text{H}\}$ NMR-DEPT135 spectrum of ligand **L2**

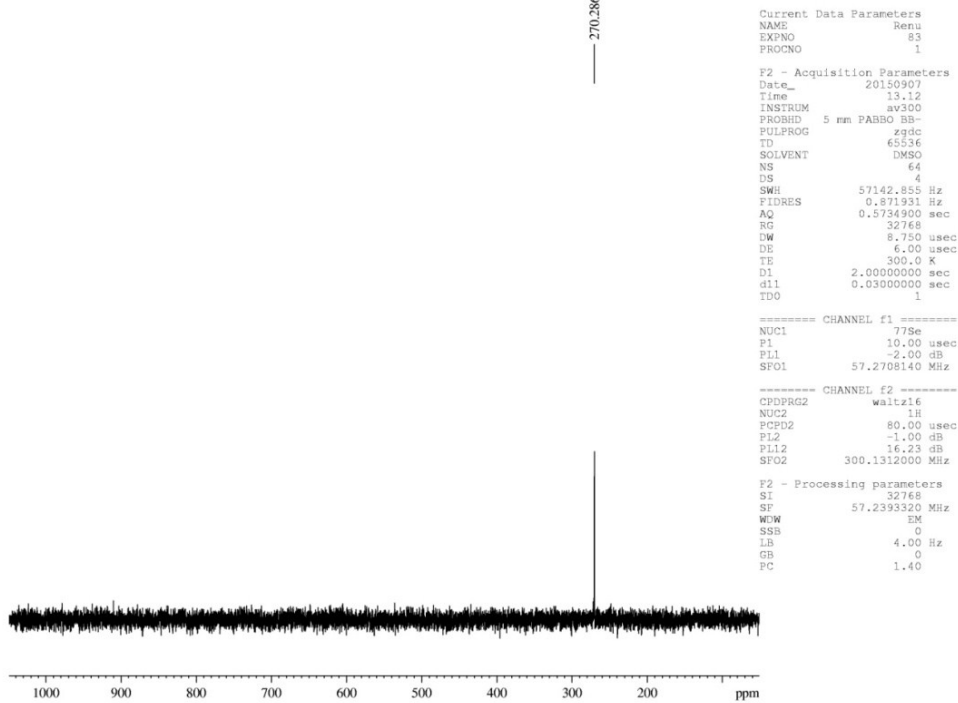


Fig. S31 $^{77}\text{Se}\{\text{H}\}$ NMR spectrum of ligand **L2**

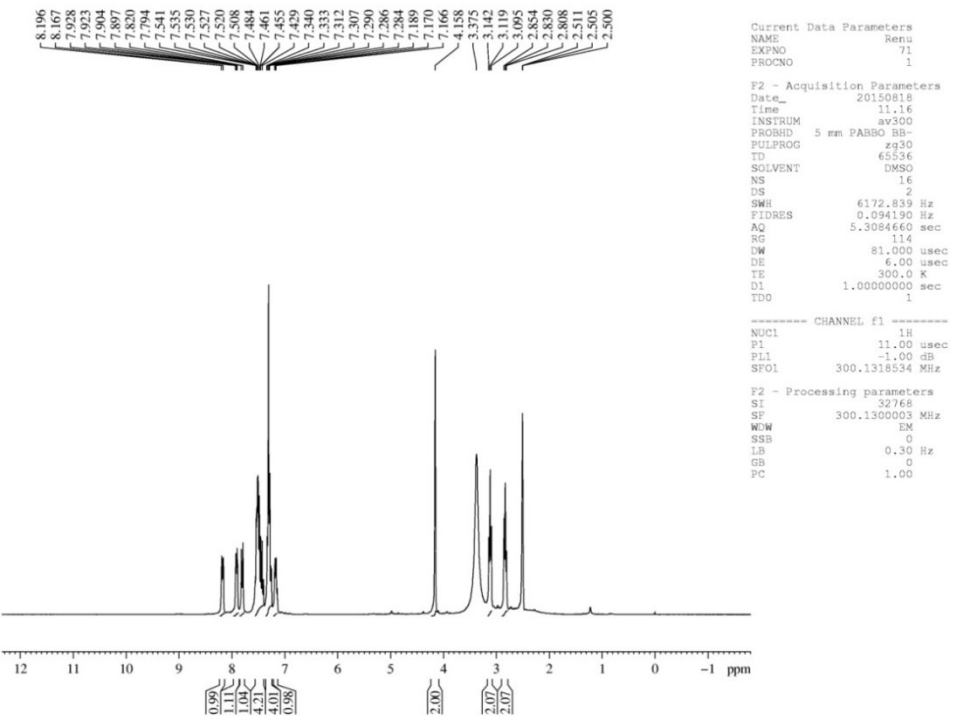


Fig. S32 ^1H NMR spectrum of ligand **L3**

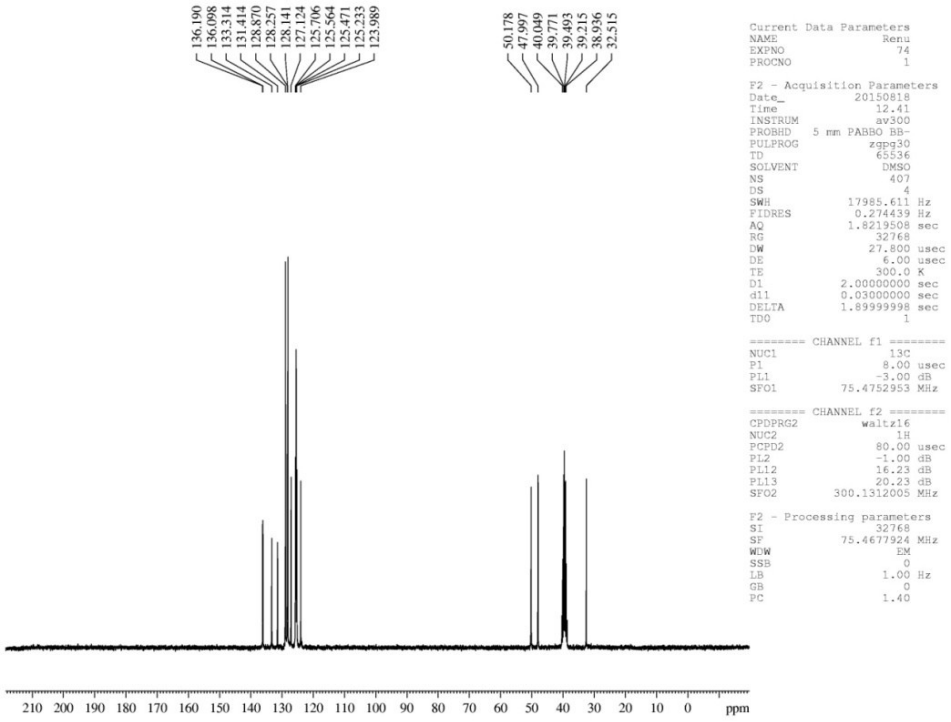


Fig. S33 $^{13}\text{C}\{^1\text{H}\}$ NMR spectrum of ligand **L3**

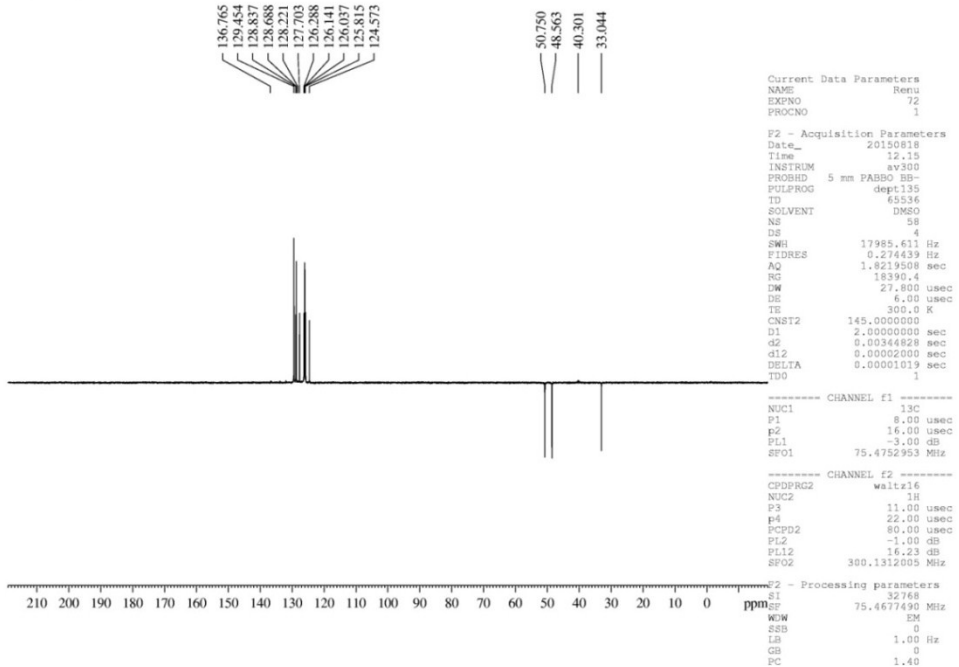


Fig. S34 $^{13}\text{C}\{^1\text{H}\}$ NMR-DEPT 135 spectrum of ligand **L3**

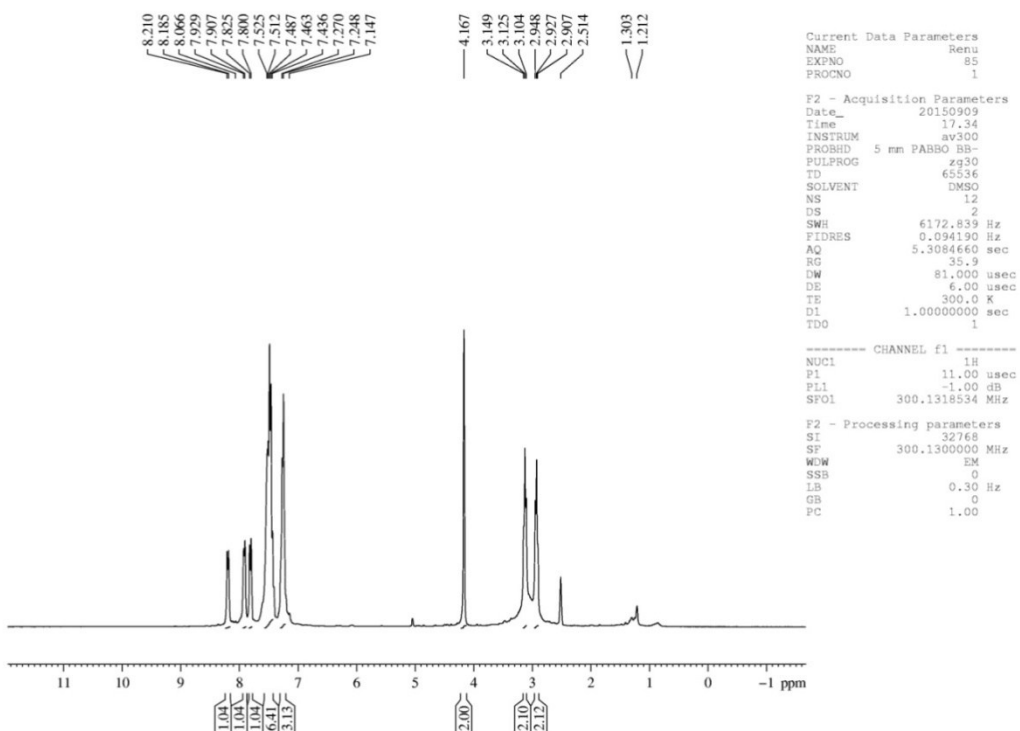


Fig. S35 ^1H NMR spectrum of ligand L4

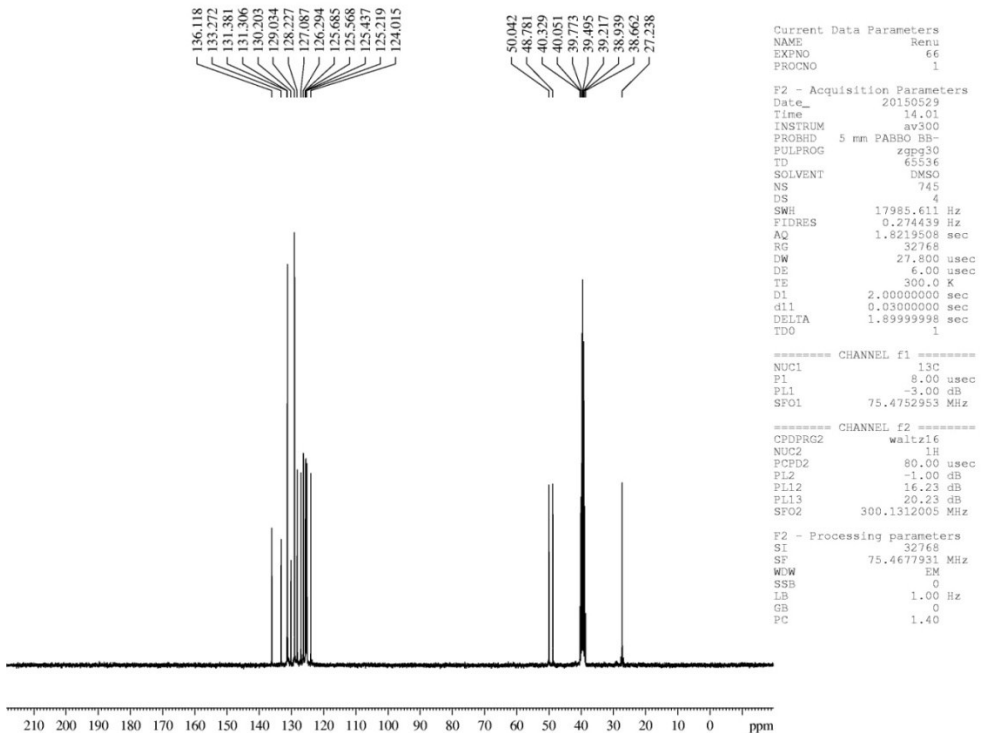


Fig. S36 $^{13}\text{C}\{^1\text{H}\}$ NMR spectrum of ligand L4

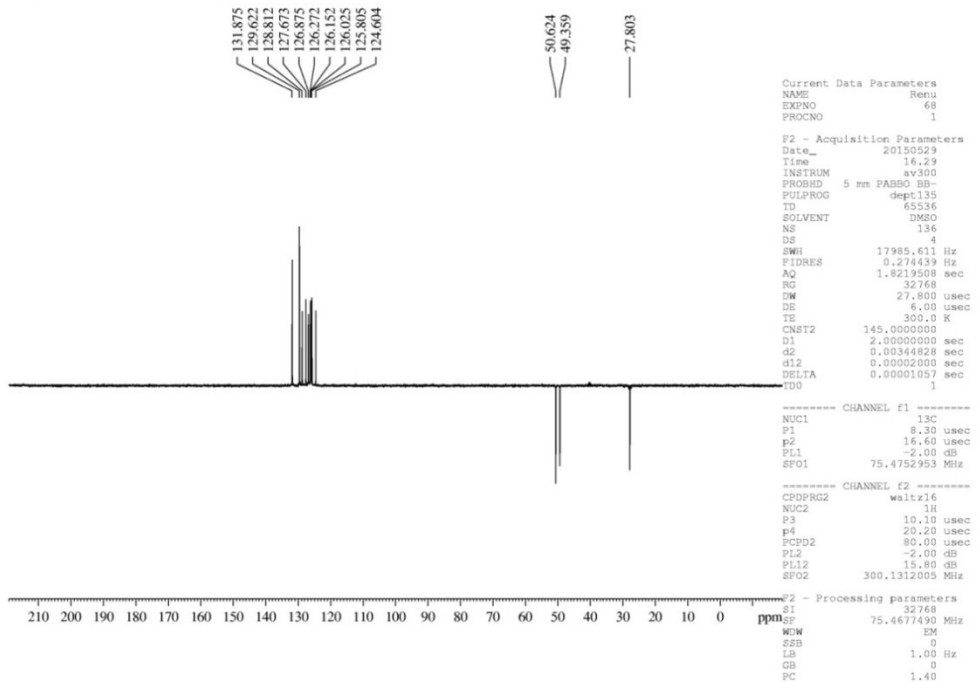


Fig. S37 $^{13}\text{C}\{\text{H}\}$ NMR-DEPT 135 spectrum of ligand L4

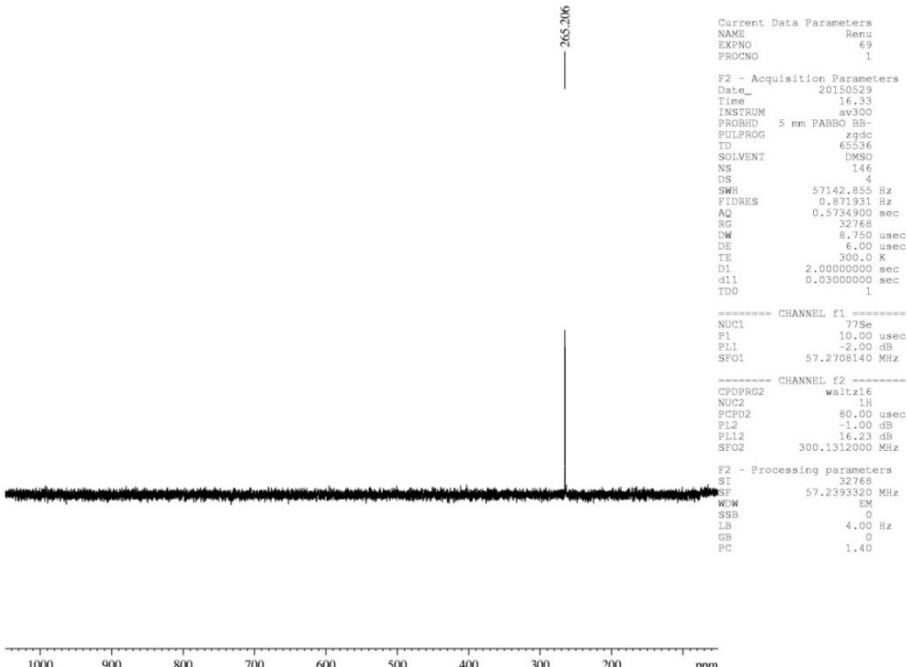


Fig. S38 $^{77}\text{Se}\{\text{H}\}$ NMR spectrum of ligand L4

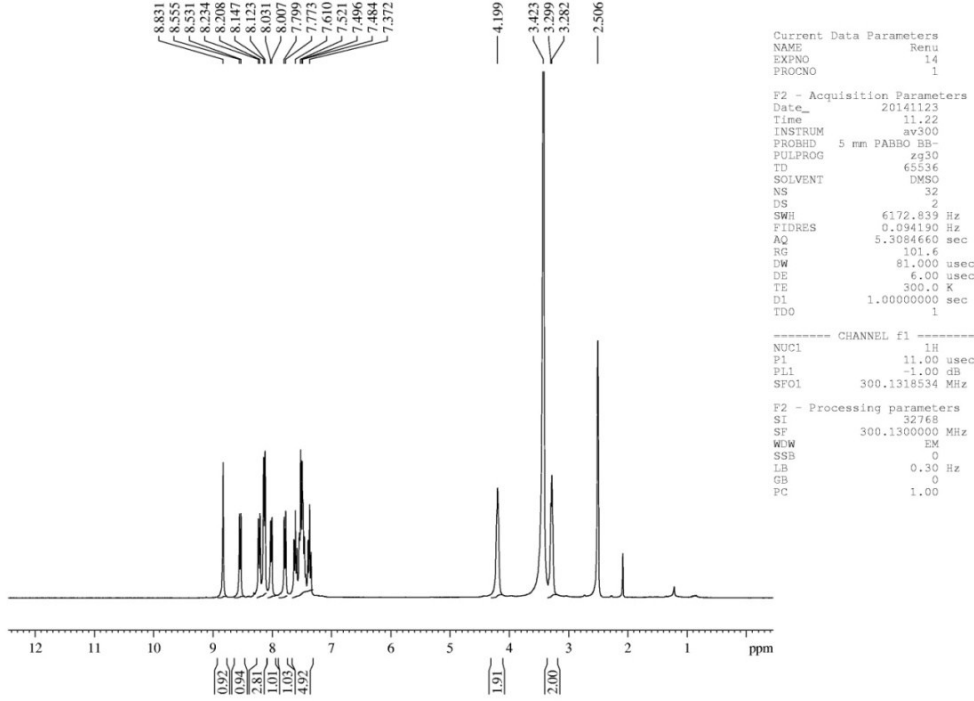


Fig. S39 ^1H NMR spectrum of complex 1

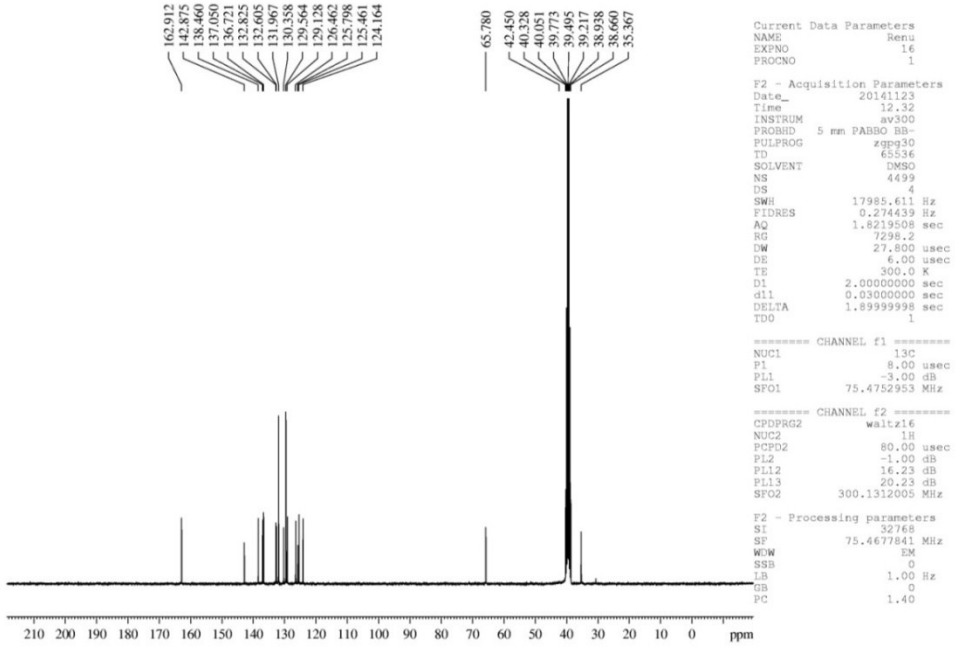


Fig. S40 $^{13}\text{C}\{^1\text{H}\}$ NMR spectrum of complex 1

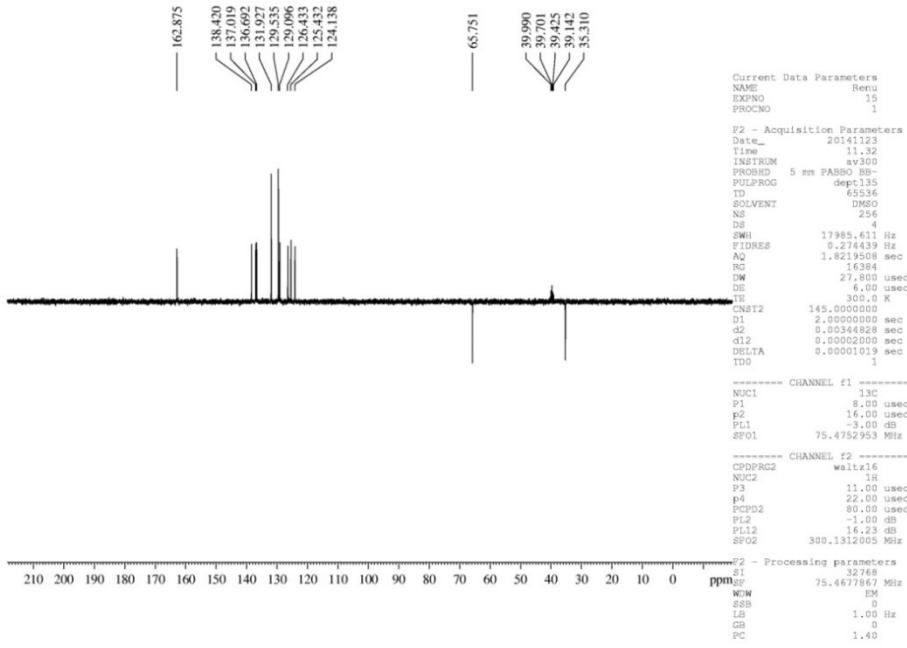


Fig. S41 $^{13}\text{C}\{\text{H}\}$ NMR-DEPT 135 spectrum of complex 1

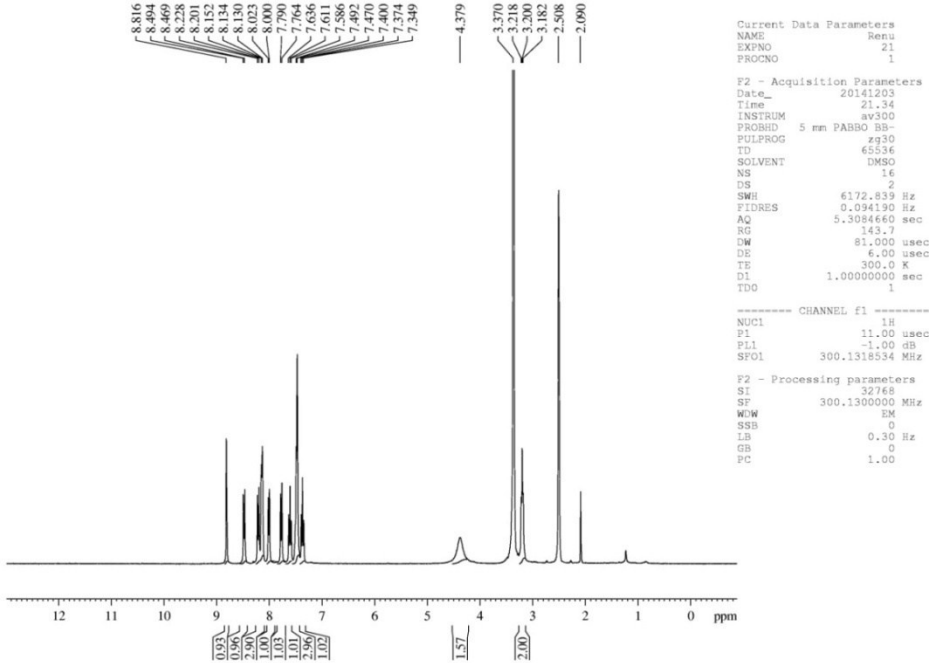


Fig. S42 ^1H NMR spectrum of complex 2

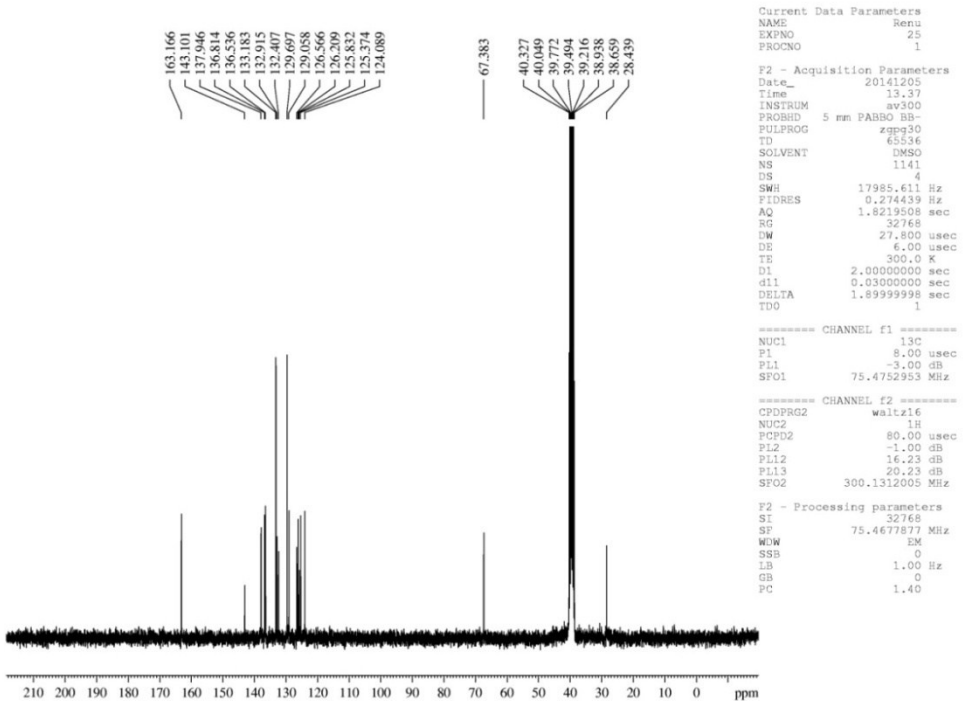


Fig. S43 $^{13}\text{C}\{^1\text{H}\}$ NMR spectrum of complex 2

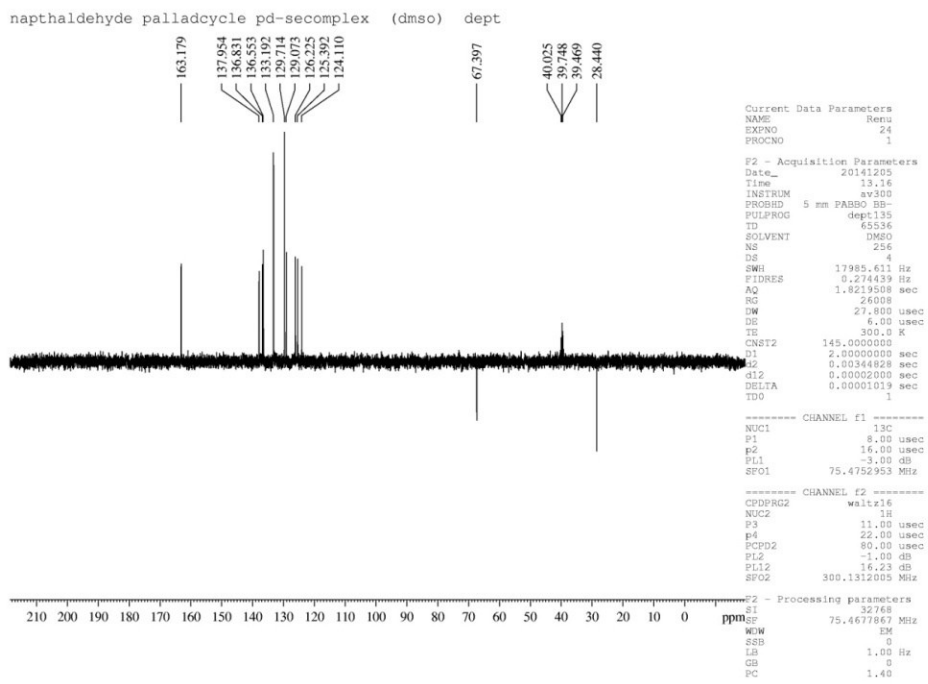


Fig. S44 $^{13}\text{C}\{^1\text{H}\}$ NMR-DEPT 135 spectrum of complex 2

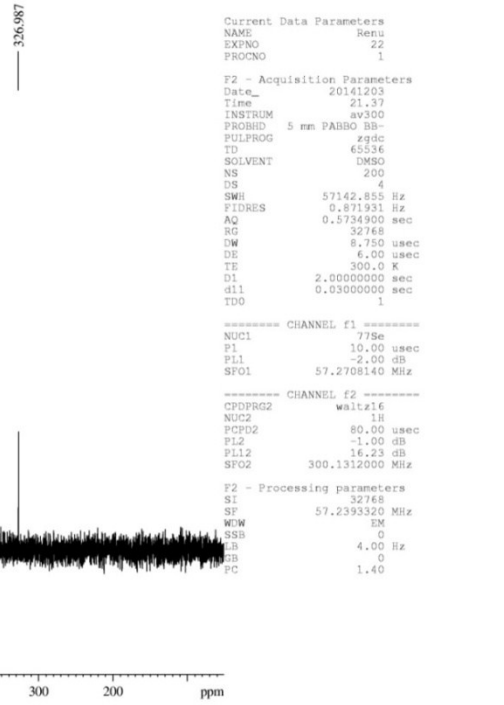


Fig. S45 $^{77}\text{Se}\{\text{H}\}$ NMR spectrum of complex 2

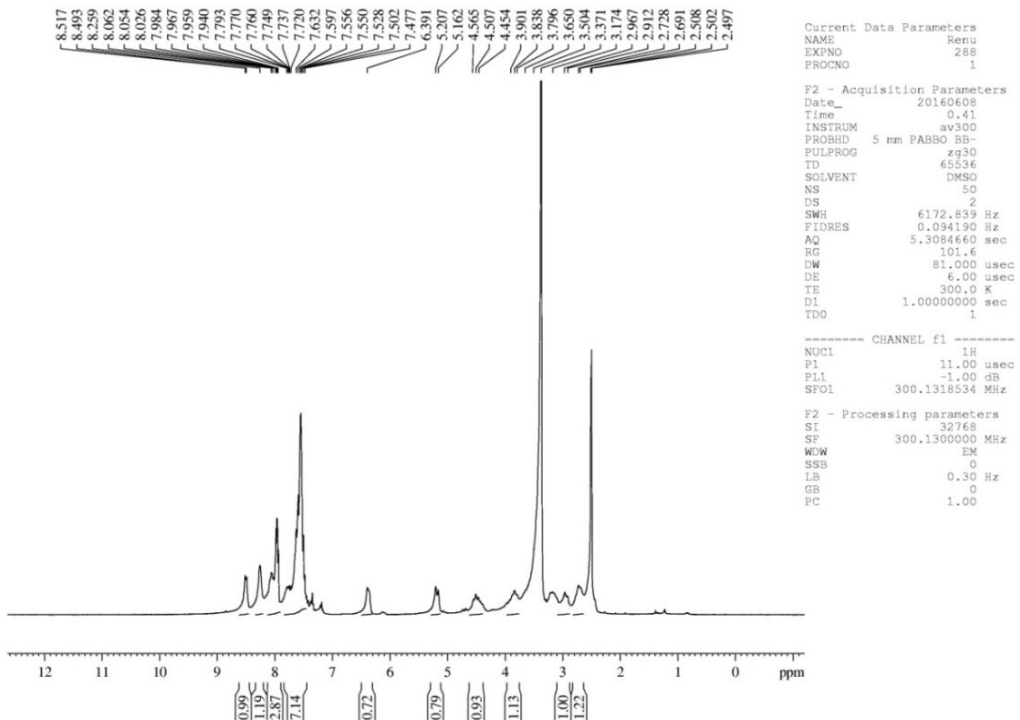


Fig. S46 ^1H NMR spectrum of complex 3

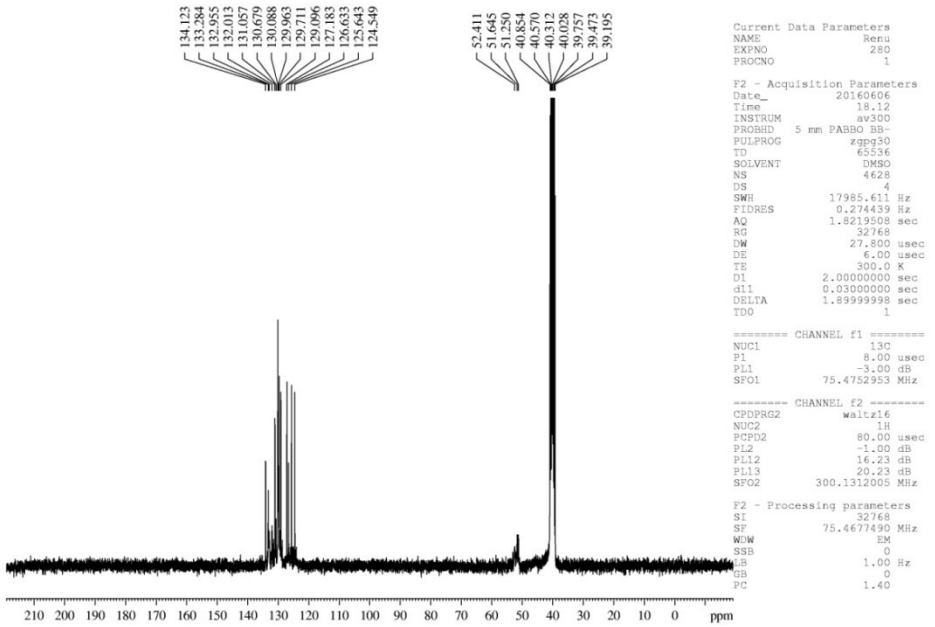


Fig. S47 $^{13}\text{C}\{\text{H}\}$ NMR spectrum of complex 3

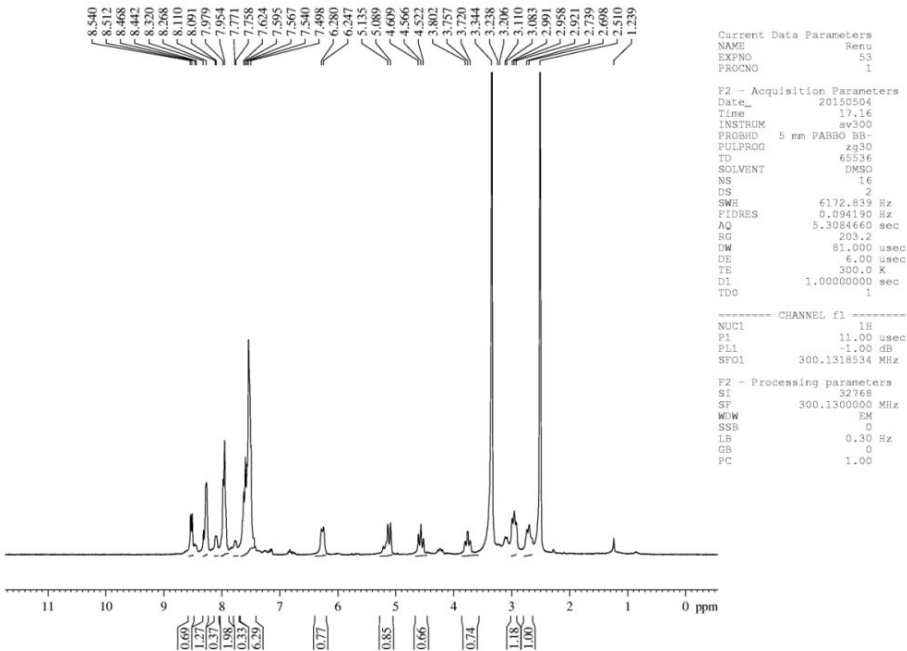


Fig. S48 ^1H NMR spectrum of complex 4

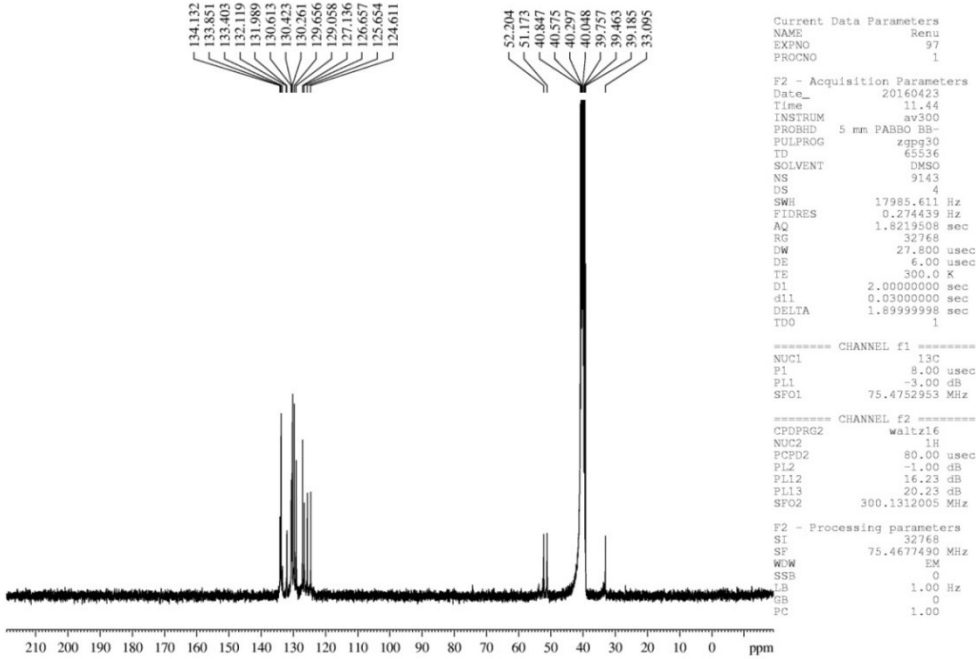


Fig. S49 $^{13}\text{C}\{\text{H}\}$ NMR spectrum of complex 4

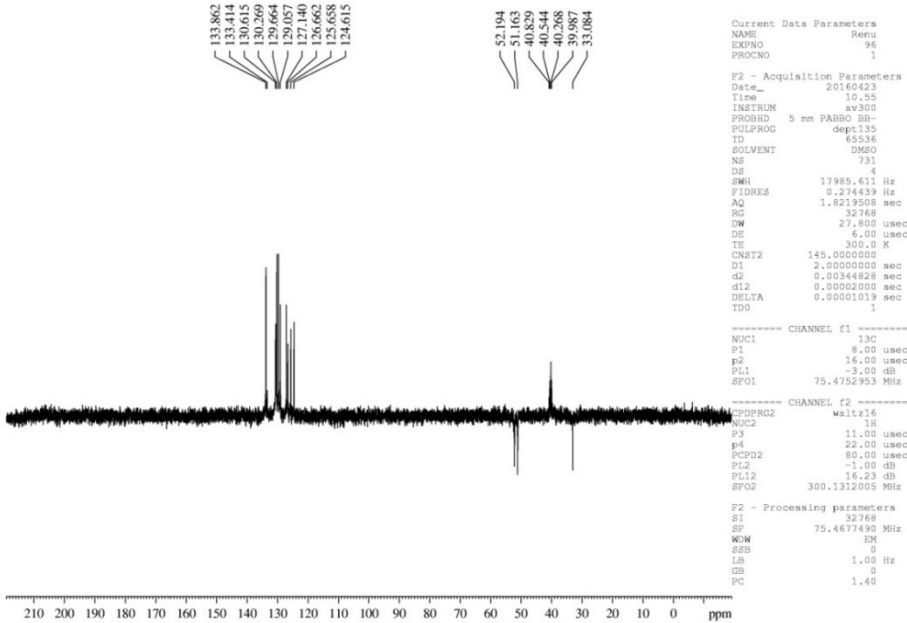


Fig. S50 $^{13}\text{C}\{\text{H}\}$ NMR-DEPT 135 spectrum of complex 4

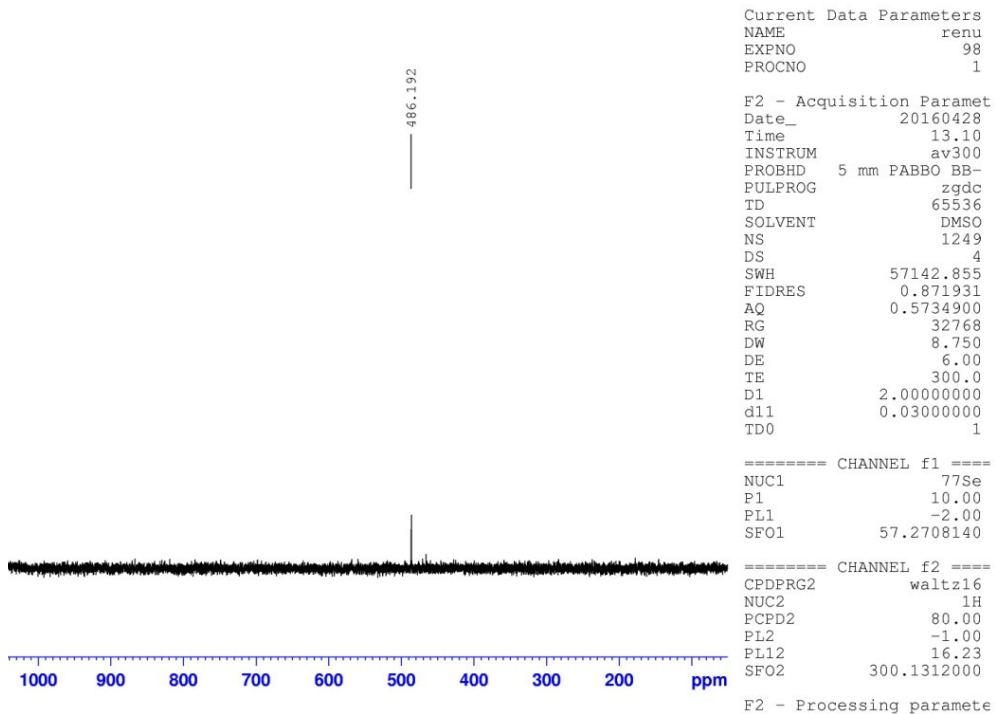


Fig. S51 $^{77}\text{Se}\{{}^1\text{H}\}$ NMR spectrum of complex 4

NMR Data of products of Sonogashira coupling reaction (1a-13a):

4-(Phenylethynyl)benzaldehyde (1a, 11a):² Light yellow solid. ^1H NMR (300 MHz, CDCl_3 , 25 °C, TMS); δ (ppm): 7.35-7.37 (m, 3H), 7.54-7.57 (m, 2H), 7.66 (d, 2H, J = 8.1 Hz), 7.85 (d, 2H, J = 8.1 Hz), 10.01 (s, 1H).

4-(Phenylethynyl)benzonitrile (2a):³ Yellow solid. ^1H NMR (300 MHz, CDCl_3 , 25 °C, TMS); δ (ppm): 7.36-7.41 (m, 3H), 7.54-7.62 (m, 2H), 7.66-7.71 (m, 4H).

(4-Acetylphenyl)phenylacetylene (3a):³ White solid. ^1H NMR (300 MHz, CDCl_3 , 25 °C, TMS); δ (ppm): 2.62 (s, 3H), 7.36-7.38 (m, 3H), 7.54-7.59 (m, 2H), 7.63 (d, J = 8.4 Hz, 2H), 7.95 (d, J = 8.4 Hz, 2H).

1-Nitro-4-(phenylethynyl)benzene (4a):³ Light-yellow solid. ^1H NMR (300 MHz, CDCl_3 , 25 °C, TMS); δ (ppm): 7.36-7.39 (m, 3H), 7.54-7.56 (m, 2H), 7.64-7.66 (m, 2H), 8.22 (d, J = 8.7 Hz, 2H)

1,2-Diphenylethyne (5a):² White solid. ^1H NMR (300 MHz, CDCl_3 , 25 °C, TMS); δ (ppm): 7.29-7.35 (m, 6H), 7.51-7.54 (m, 4H).

1-Methyl-4-(phenylethynyl)benzene (6a, 13a):² White solid. ¹H NMR (300 MHz, CDCl₃, 25 °C, TMS); δ (ppm): 2.37 (s, 3H), 7.15 (d, J = 7.2 Hz, 2H), 7.32-7.34 (m, 3H), 7.43 (d, J = 8.1 Hz 2H,), 7.51-7.53 (m, 2H).

2-(Phenylethynyl)benzaldehyde (7a):² Yellow solid. ¹H NMR (300 MHz, CDCl₃, 25 °C, TMS); δ (ppm): 7.34-7.39 (m, 3H), 7.44 (br, 1H), 7.55-7.60 (m, 3H), 7.64 (d, J = 7.8 Hz, 1H,), 7.95 (d, J = 7.8 Hz, 1H), 10.65 (s, 1H).

(2-Phenylethynyl)pyridine (8a):³ Yellow oil. ¹H NMR (300 MHz, CDCl₃, 25 °C, TMS); δ (ppm): 7.23-7.26 (m, 1H), 7.35-7.38 (m, 3H), 7.51-7.54 (m, 1H), 7.60-7.62 (m, 2H), 7.70 (m, 1H), 8.62 (d, J = 4.2 Hz, 1H).

2,6-bis(phenylethynyl)pyridine (9a):⁴ Yellow solid. ¹H NMR (300 MHz, CDCl₃, 25 °C, TMS); δ (ppm): 7.31-7.36 (m, 6H), 7.41-7.43 (m, 2H), 7.59-7.63 (m, 5H).

(2-Phenylethynyl)thiophene (10a):⁵ Yellow oil. ¹H NMR (300 MHz, CDCl₃, 25 °C, TMS): δ (ppm): 7.54-7.58 (m, 2H), 7.32-7.41 (m, 5H), 7.04-7.07 (m, 1H).

1-Methoxy-4-(phenylethynyl)benzene (12a):² White Solid. ¹H NMR (300 MHz, CDCl₃, 25 °C, TMS): δ (ppm): 3.81 (s, 3H), 6.92 (d, J = 9 Hz, 2H), 7.31-7.41 (m, 3H), 7.43-7.64 (m, 4H).

NMR Data of products of Suzuki-Miyaura coupling reaction (1b-9b):

4-Phenylbenzaldehyde (1b, 9b):⁶ Light yellow solid. ¹H NMR (300 MHz, CDCl₃, 25 °C, TMS); δ (ppm): 7.40-7.51 (m, 3H), 7.63-7.65 (m, 2H), 7.75 (d, J = 8.4 Hz, 2H), 7.95 (d, J = 8.4 Hz, 2H), 10.05 (s, 1H).

4-Phenylbenzonitrile (2b):⁶ Pale yellow solid. ¹H NMR (300 MHz, CDCl₃, 25 °C, TMS); δ (ppm): 7.40-7.50 (m, 3H), 7.57-7.60 (m, 2H), 7.66-7.74 (m, 4H).

4-Nitrobiphenyl (3b):⁶ Pale Yellow solid. ¹H NMR (300 MHz, CDCl₃, 25 °C, TMS); δ (ppm): 7.42-7.53 (m, 3H), 7.62 (d, J = 7.5 Hz, 2H), 7.74 (d, J = 9.0 Hz, 2H), 8.30 (d, J = 9.0 Hz, 2H).

4-Acetyl biphenyl (4b):⁶ White solid. ¹H NMR (300 MHz, CDCl₃, 25 °C, TMS); δ (ppm): 2.64 (s, 3H), 7.38-7.51 (m, 3H), 7.62-7.70 (m, 4H), 8.02 (d, J = 8.7 Hz, 2H).

Biphenyl-4-carboxylic acid (5b):⁶ White solid. ¹H NMR (300 MHz, CDCl₃, 25 °C, TMS); δ (ppm): 7.41-7.51 (m, 3H), 7.63-7.71 (m, 4H), 8.17 (d, J = 8.1 Hz, 2H).

Biphenyl (6b):⁶ White solid. ¹H NMR (300 MHz, CDCl₃, 25 °C, TMS); δ (ppm): 7.33-7.35 (m, 2H), 7.43 (t, J = 7.2 Hz, 4H), 7.58 (d, J = 7.2 Hz, 4H).

4-Methylbiphenyl (7b):⁶ Colorless solid. ¹H NMR (300 MHz, CDCl₃, 25°C, TMS); δ (ppm): 2.39 (s, 3H), 7.23 (d, J = 7.8 Hz, 2H), 7.28-7.34 (m, 1H), 7.38-7.44 (m, 2H), 7.49 (d, J = 8.1 Hz, 2H), 7.56-7.59 (m, 2H).

4-Methoxybiphenyl (8b):⁶ White solid. ¹H NMR (300 MHz, CDCl₃, 25°C, TMS); δ (ppm): 3.78 (s, 3H), 6.93 (d, *J* = 8.7 Hz, 2H), 7.28-7.30 (m, 1H), 7.40 (t, *J* = 7.2 Hz, 2H), 7.49-7.55 (m, 4H).

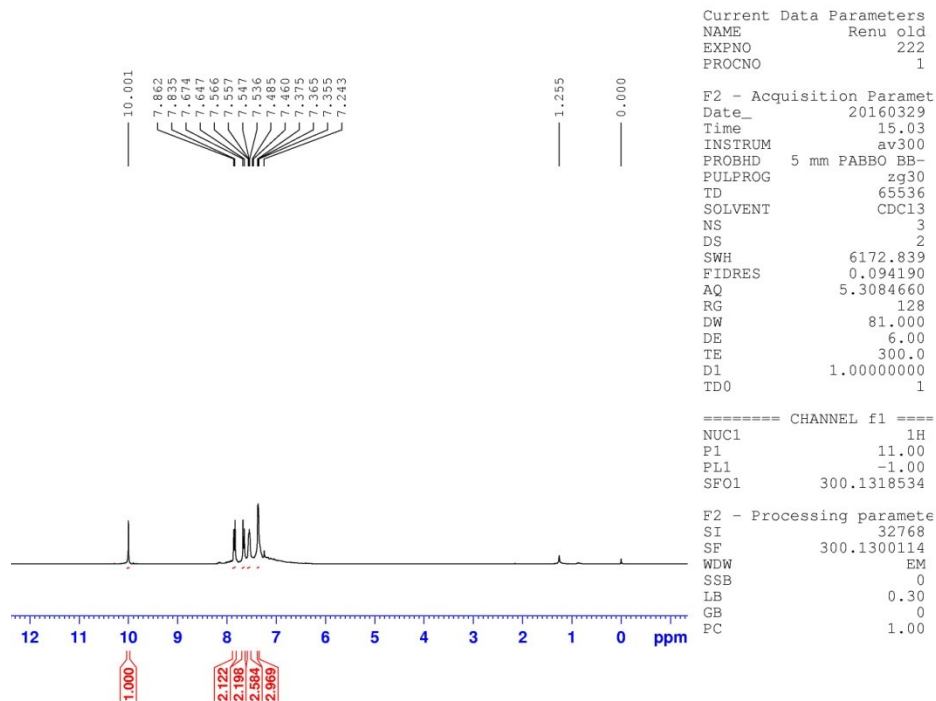


Fig. S52 ¹H NMR spectrum of 1a

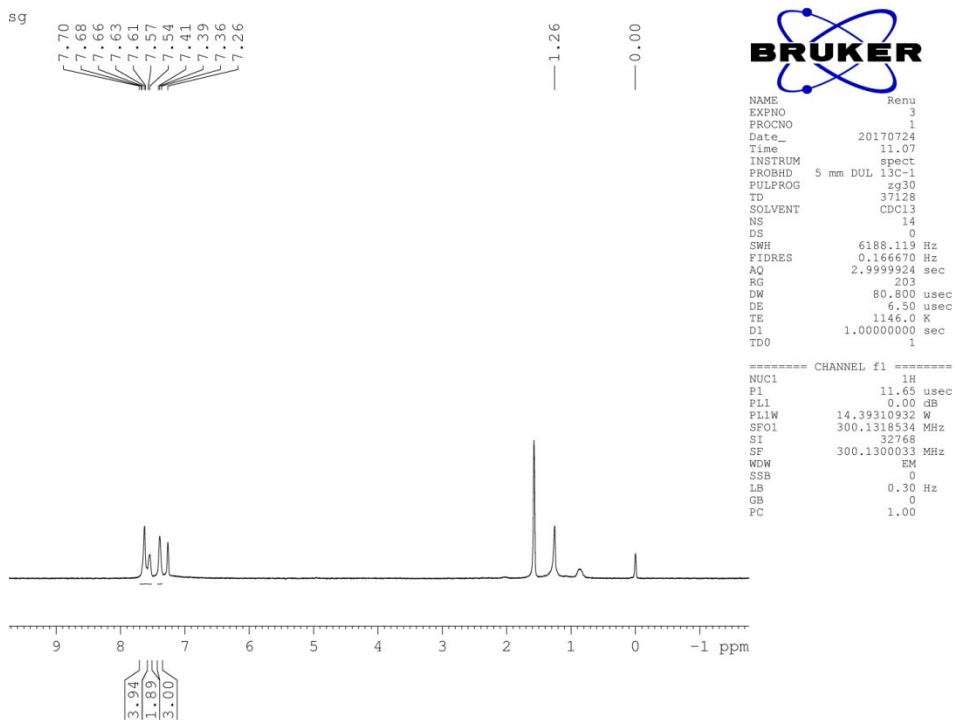


Fig. S53 ¹H NMR spectrum of 2a

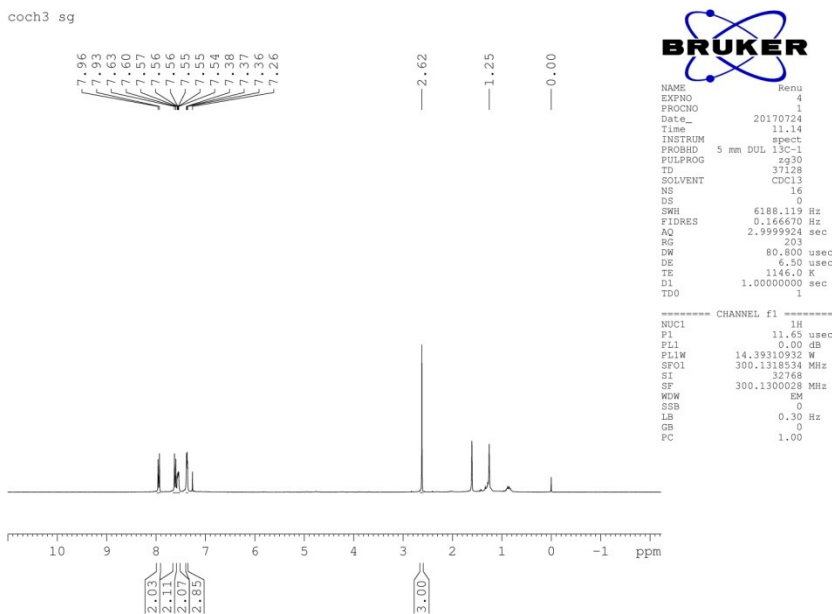


Fig. S54 ^1H NMR spectrum of **3a**

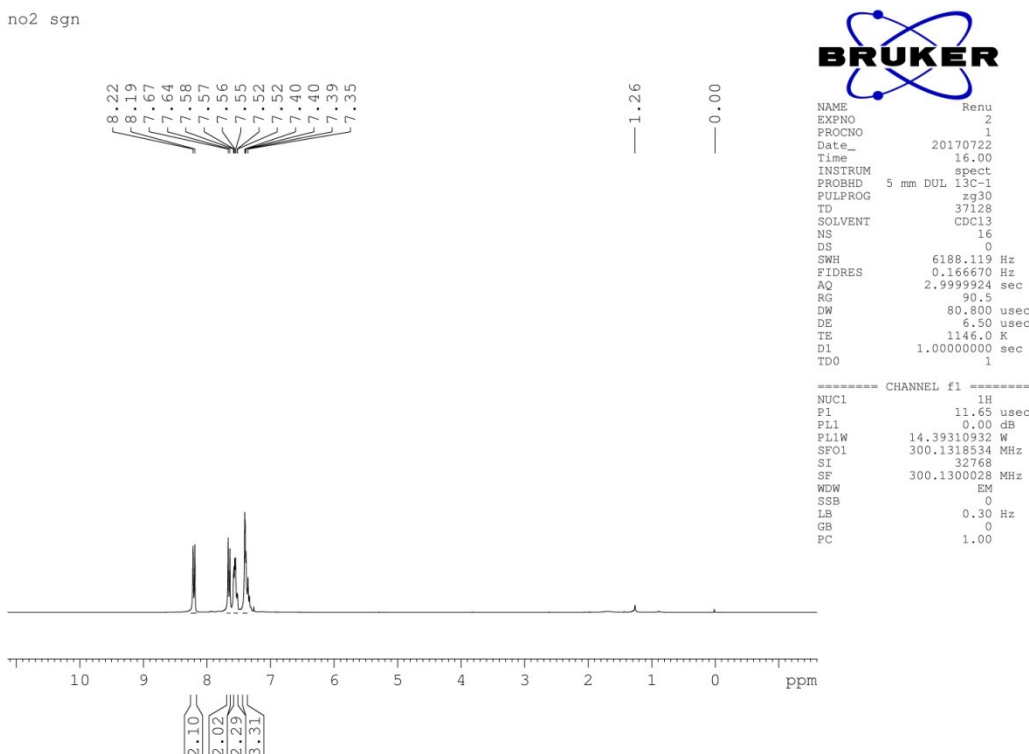


Fig. S55 ^1H NMR spectrum of **4a**

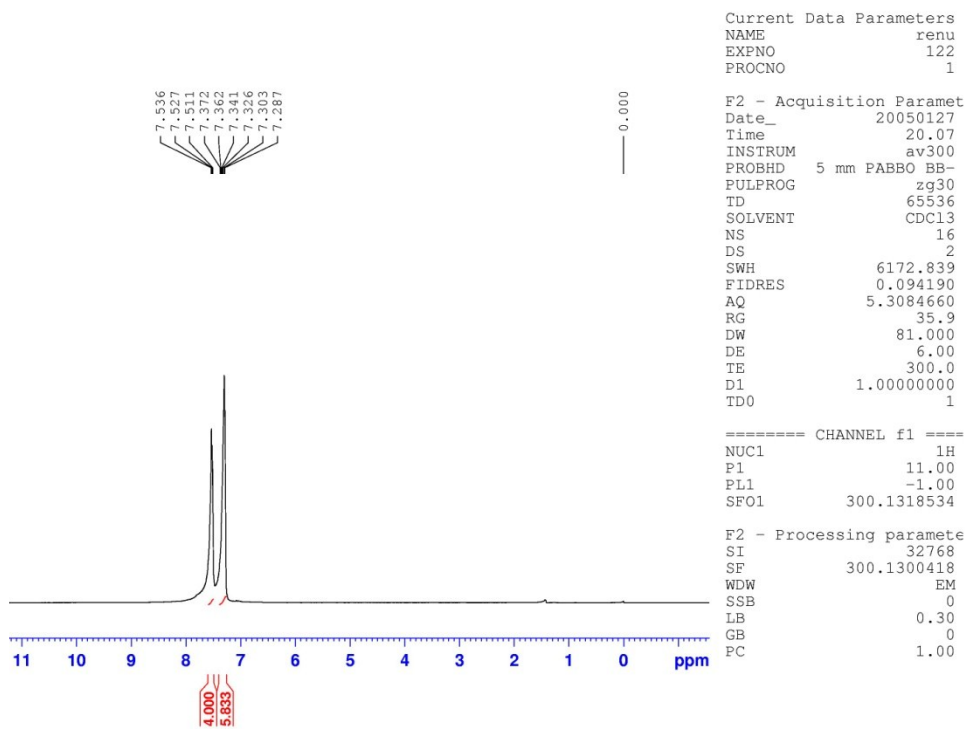


Fig. S56 ^1H NMR spectrum of **5a**

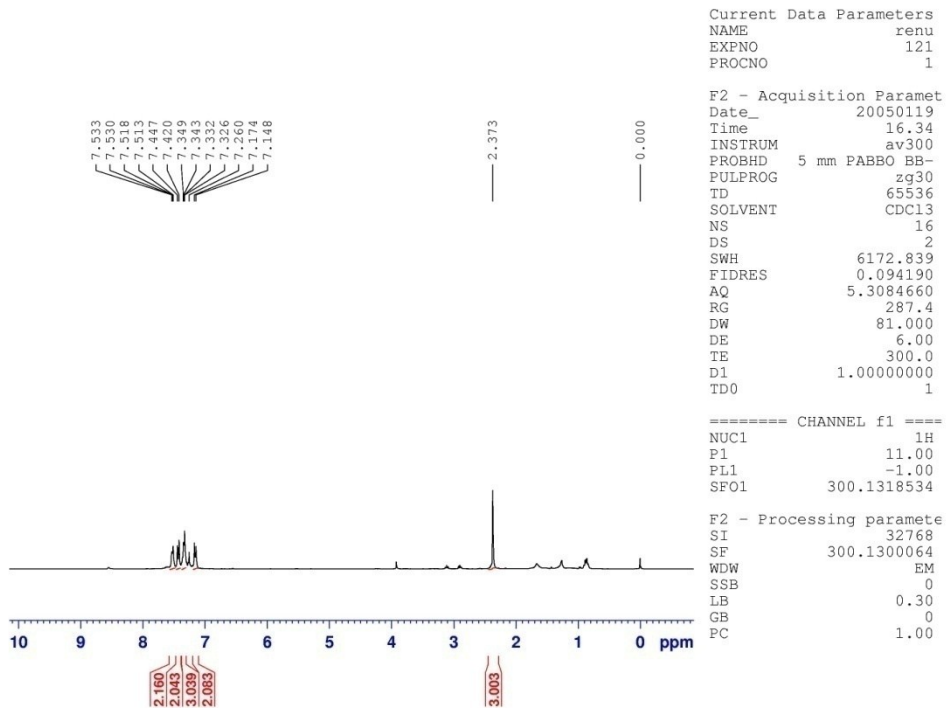


Fig. S57 ^1H NMR spectrum of **6a**

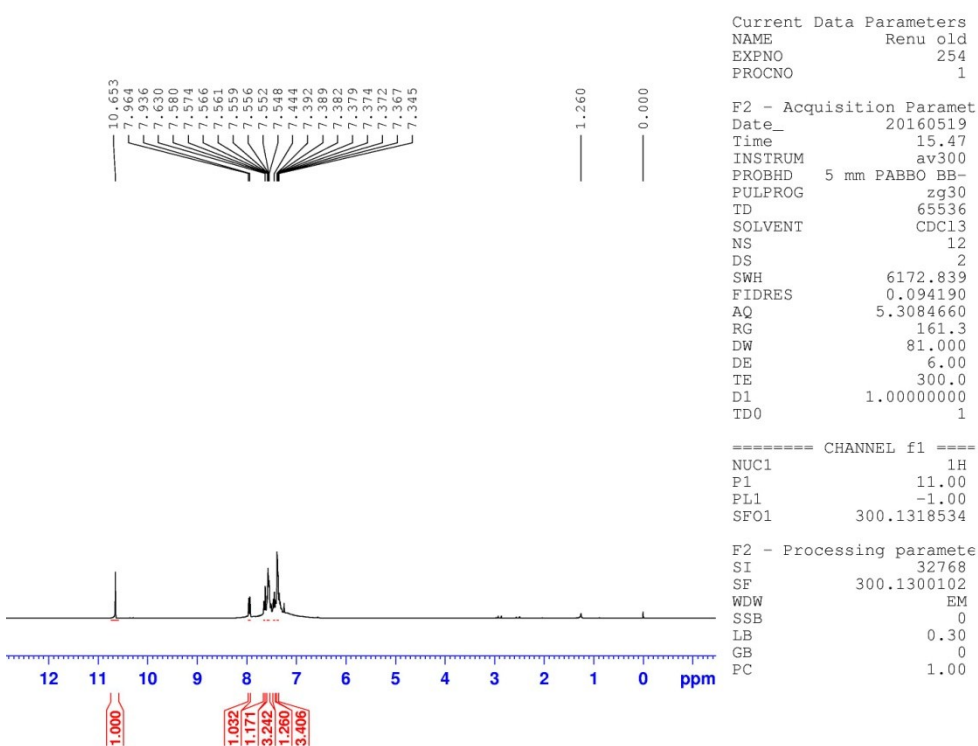


Fig. S58 ^1H NMR spectrum of 7a

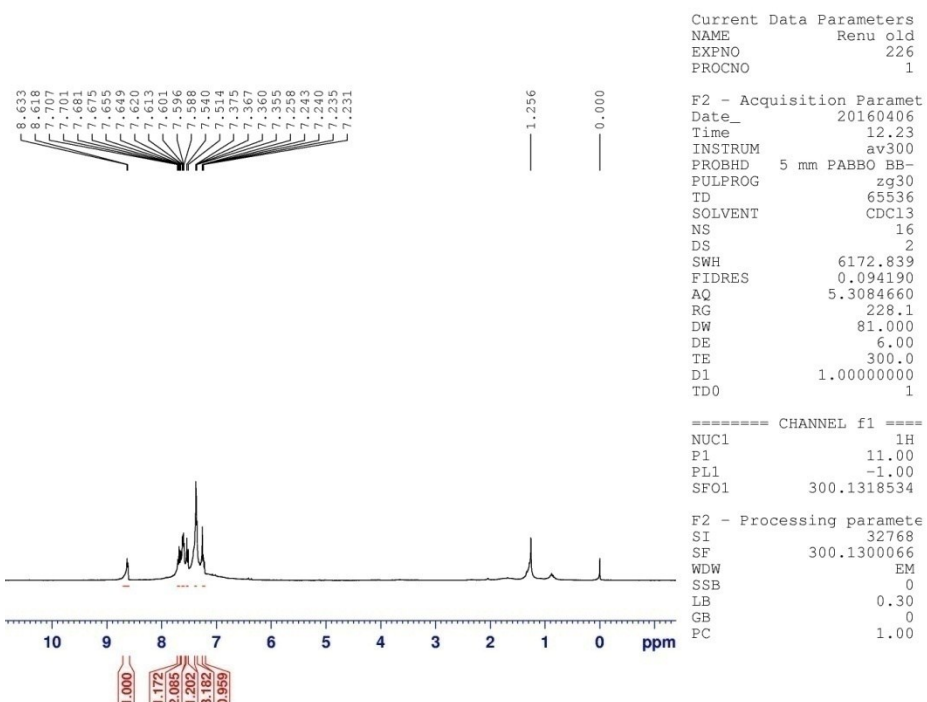


Fig. S59 ^1H NMR spectrum of 8a

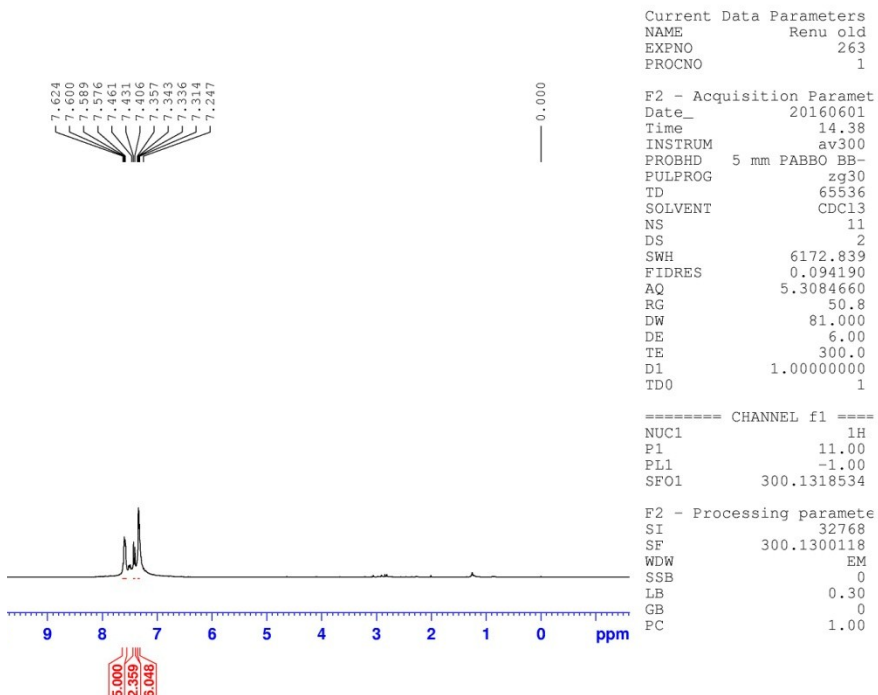


Fig. S60 ¹H NMR spectrum of **9a**

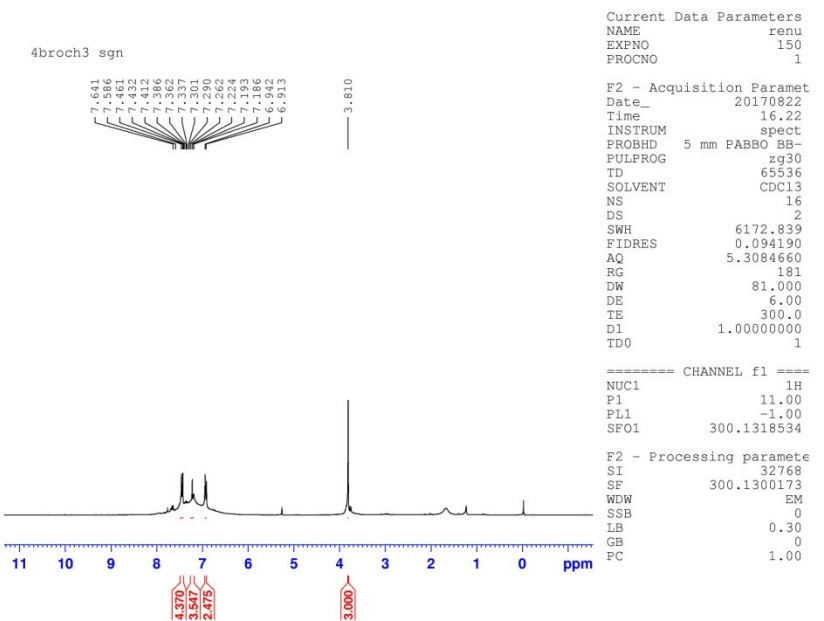


Fig. S61 ¹H NMR spectrum of **12a**

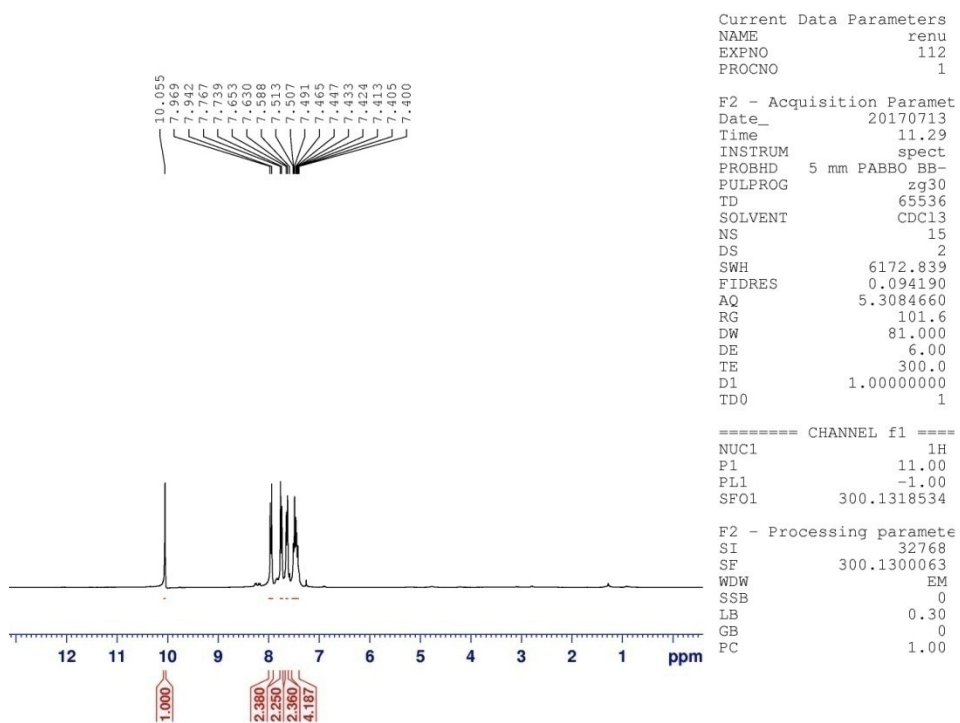


Fig. S62 ¹H NMR spectrum of 1b

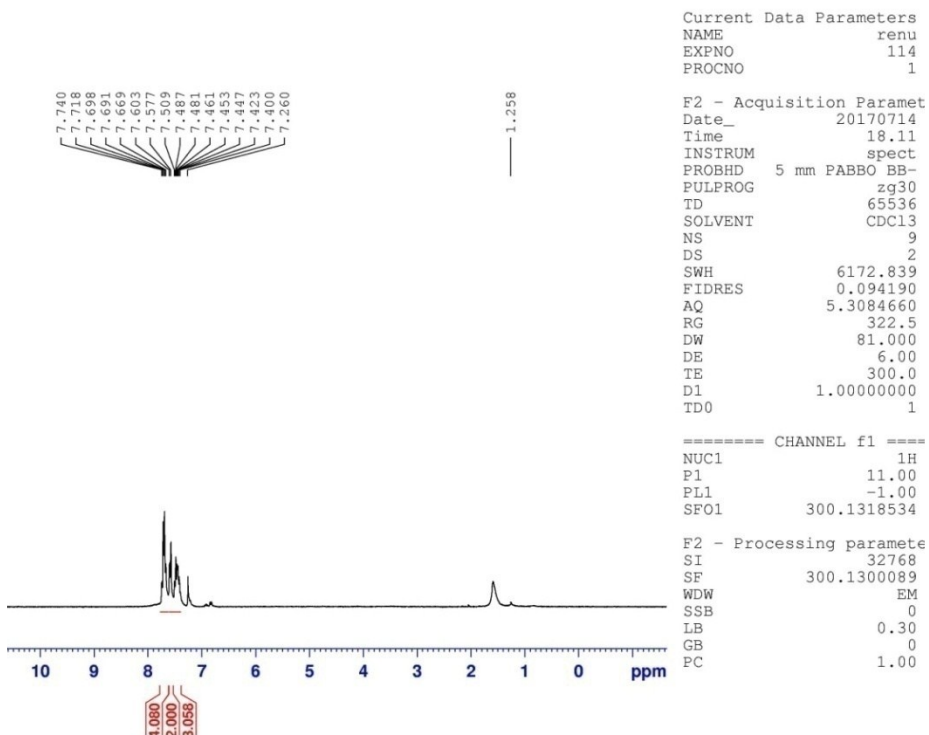


Fig. S63 ¹H NMR spectrum of 2b

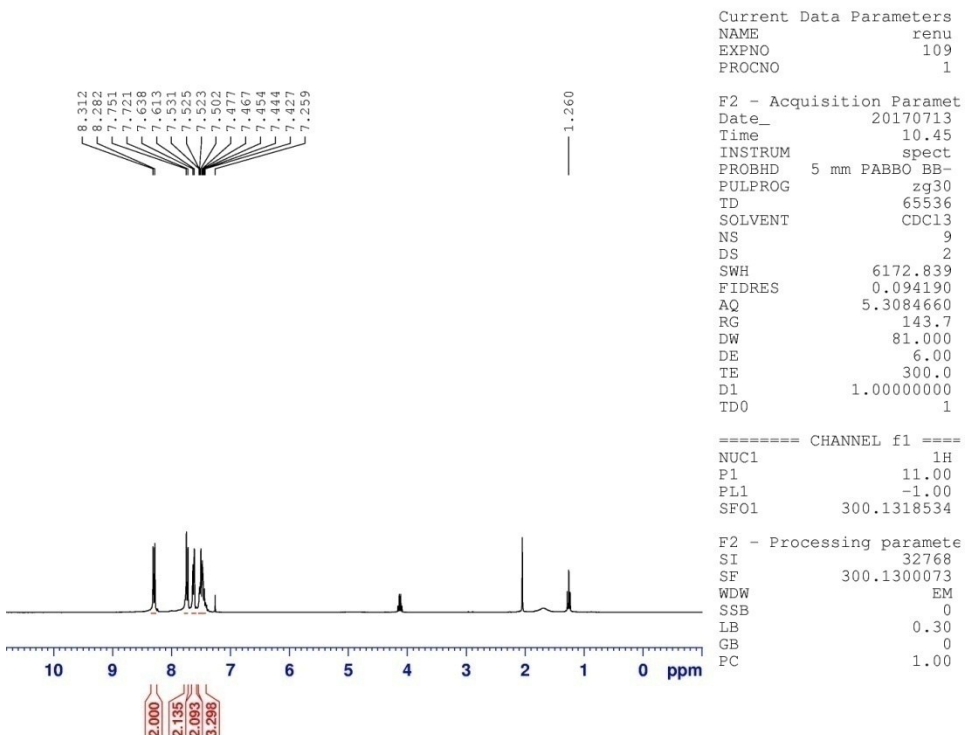


Fig. S64 ^1H NMR spectrum of **3b**

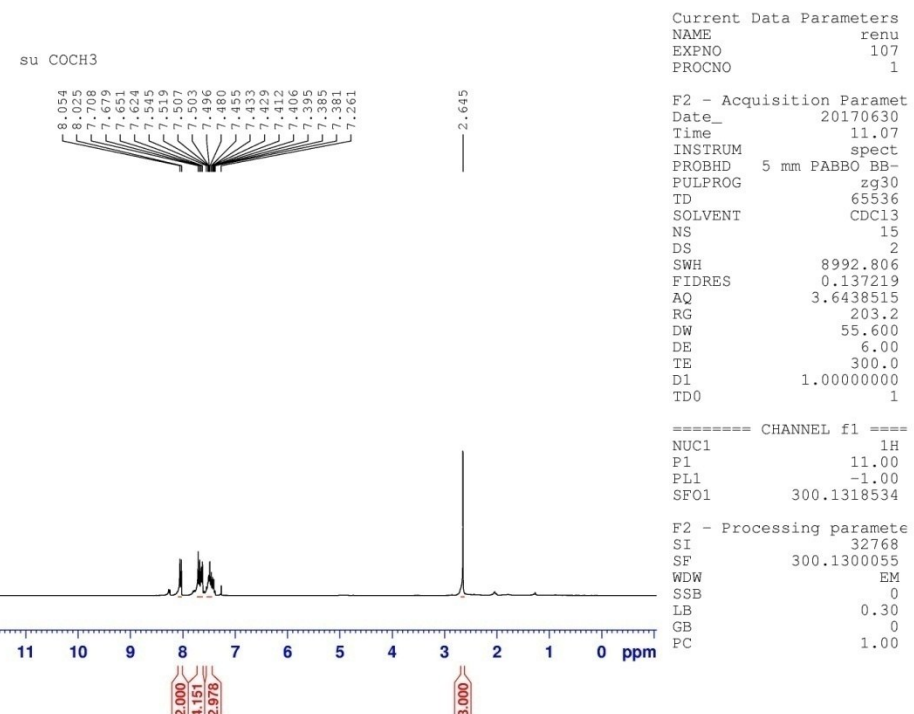


Fig. S65 ^1H NMR spectrum of **4b**

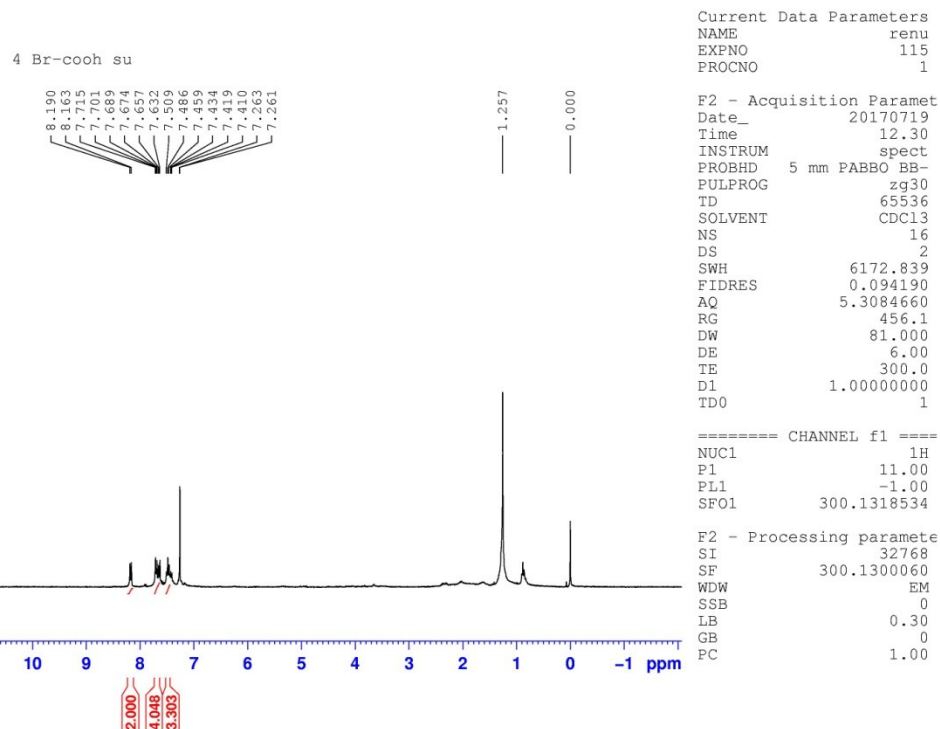


Fig. S66 ^1H NMR spectrum of **5b**

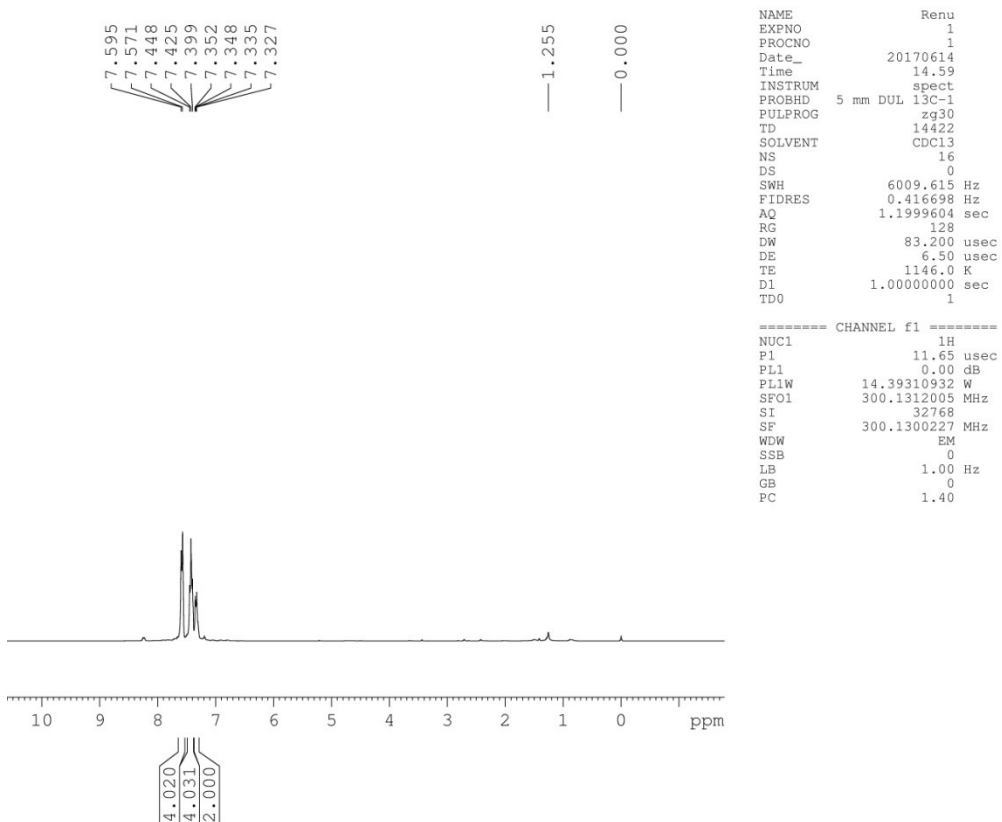


Fig. S67 ^1H NMR spectrum of **6b**

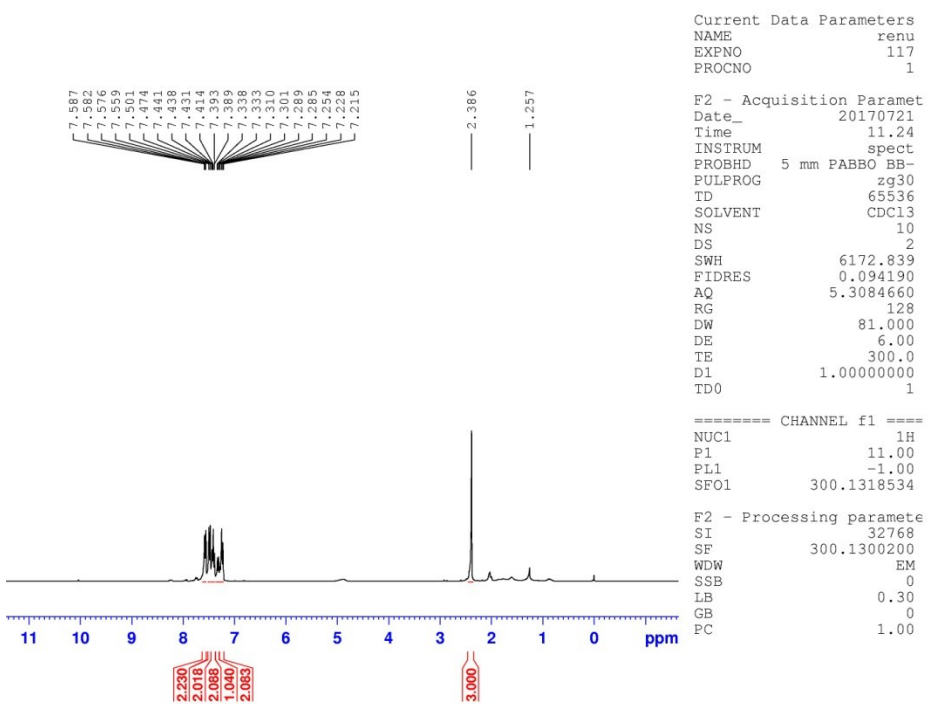


Fig. S68 ^1H NMR spectrum of **7b**

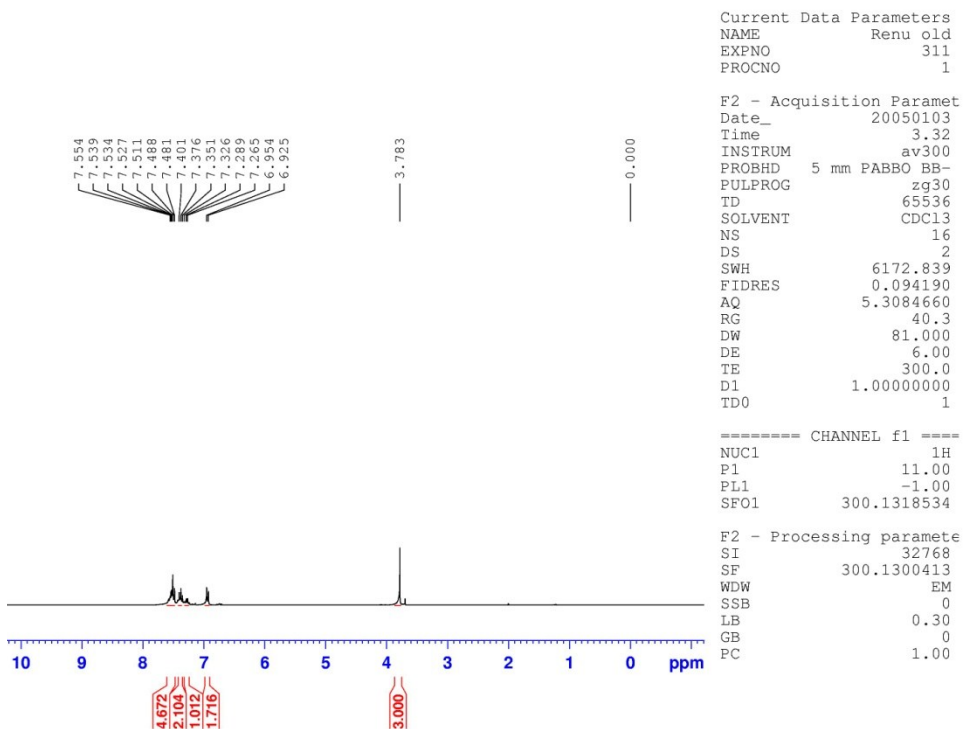


Fig. S69 ^1H NMR spectrum of **8b**

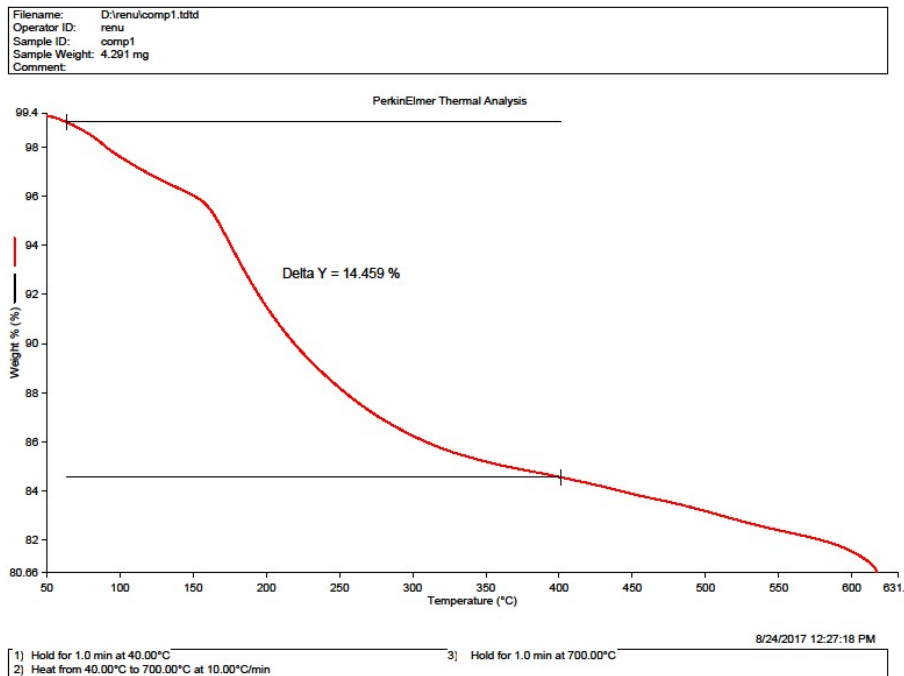


Fig. S70 TGA of NPs obtained from **1** after SMC

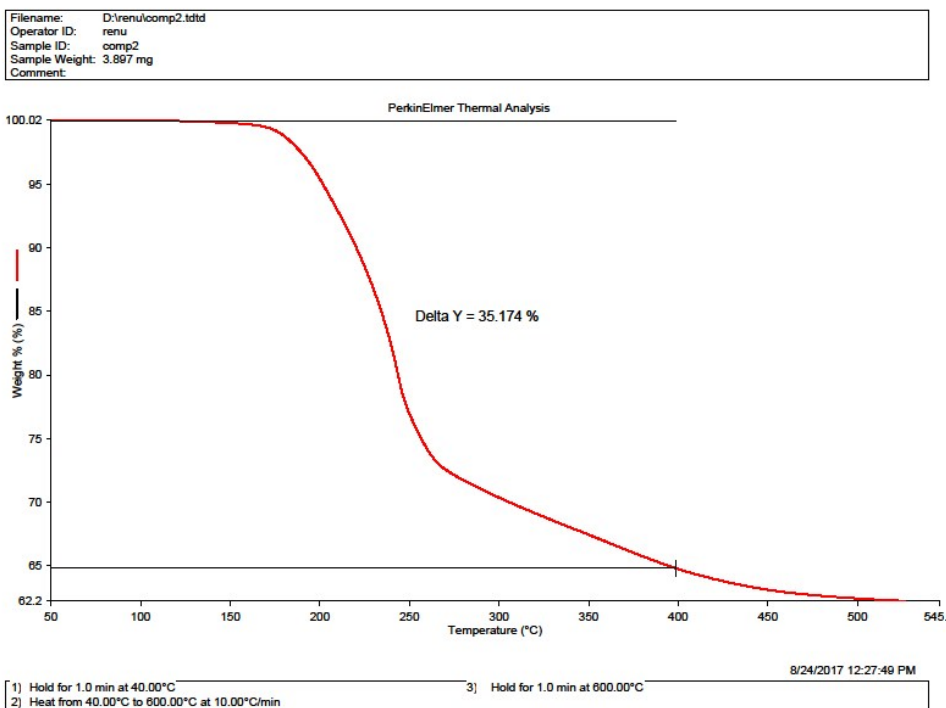


Fig. S71 TGA of NPs obtained from **2** after SMC

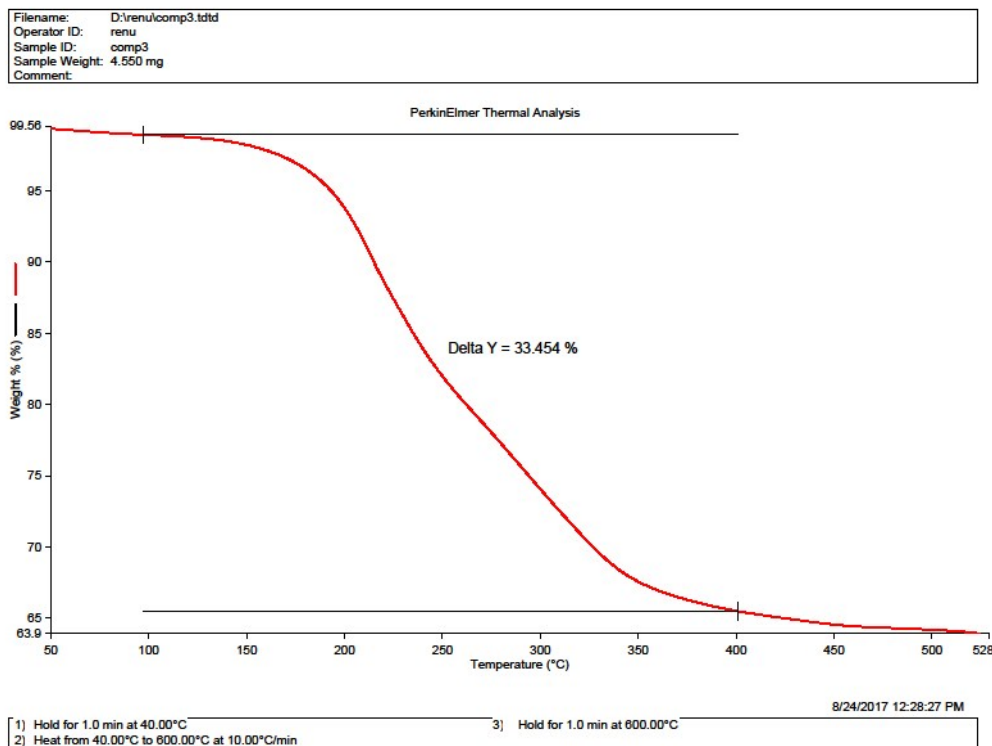


Fig. S72 TGA of NPs obtained from **3** after SMC

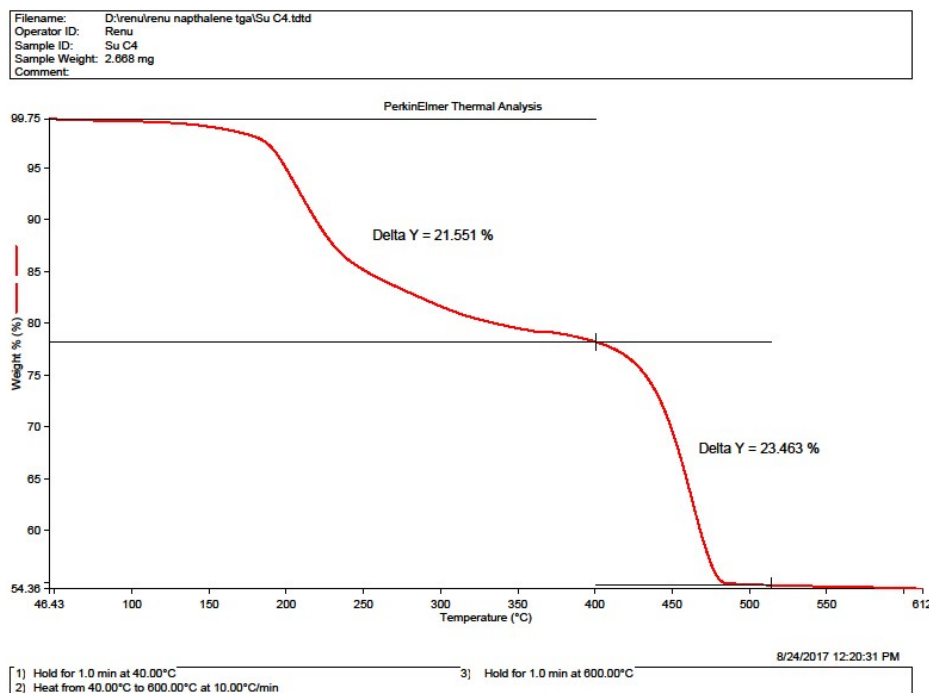


Fig. S73 TGA of NPs obtained from **4** after SMC

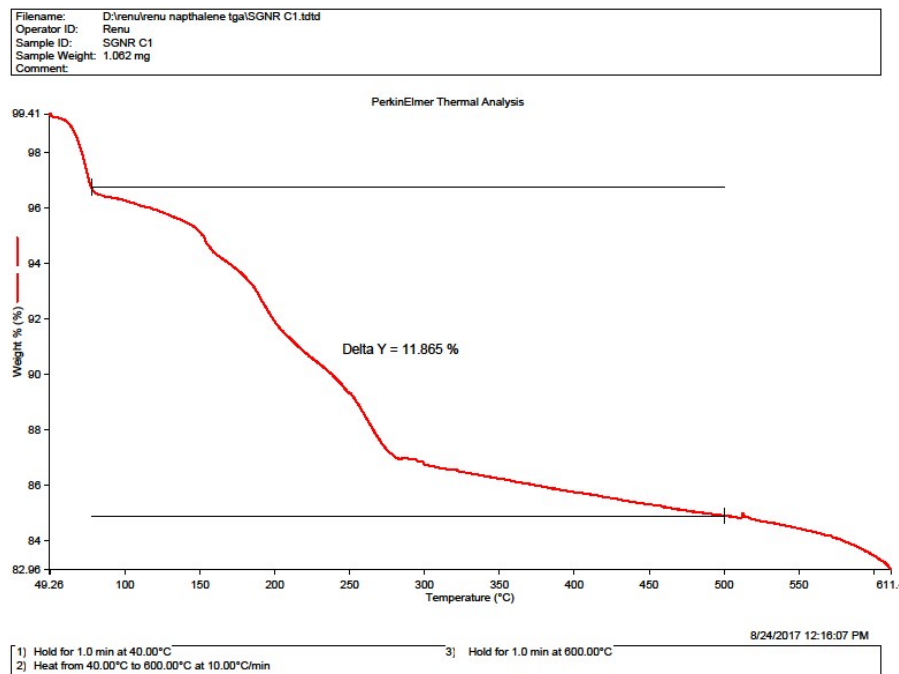


Fig. S74 TGA of NPs obtained from **1** after Sonogashira coupling reaction

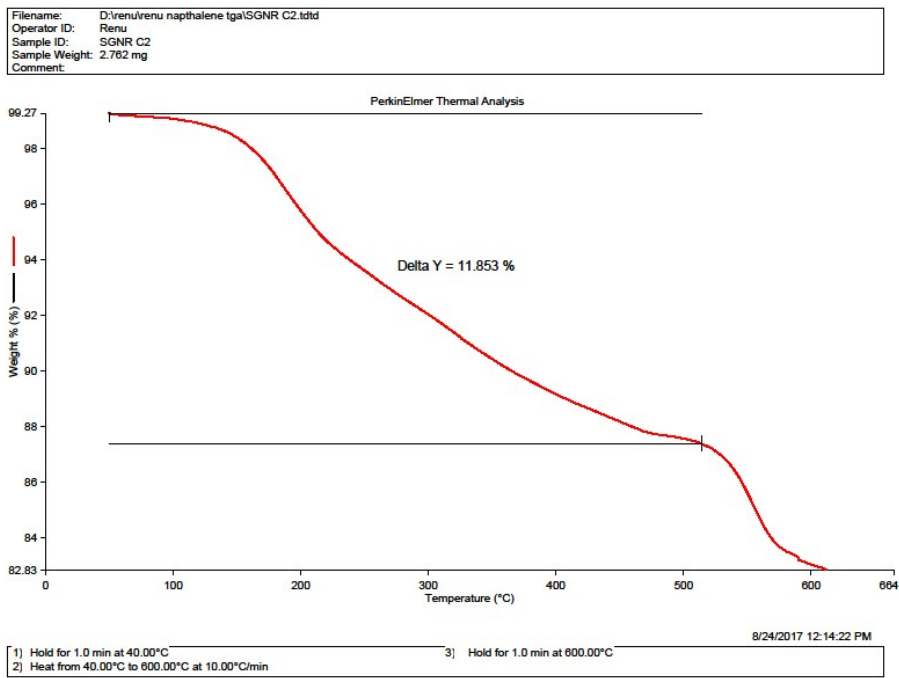


Fig. S75 TGA of NPs obtained from **2** after Sonogashira coupling reaction

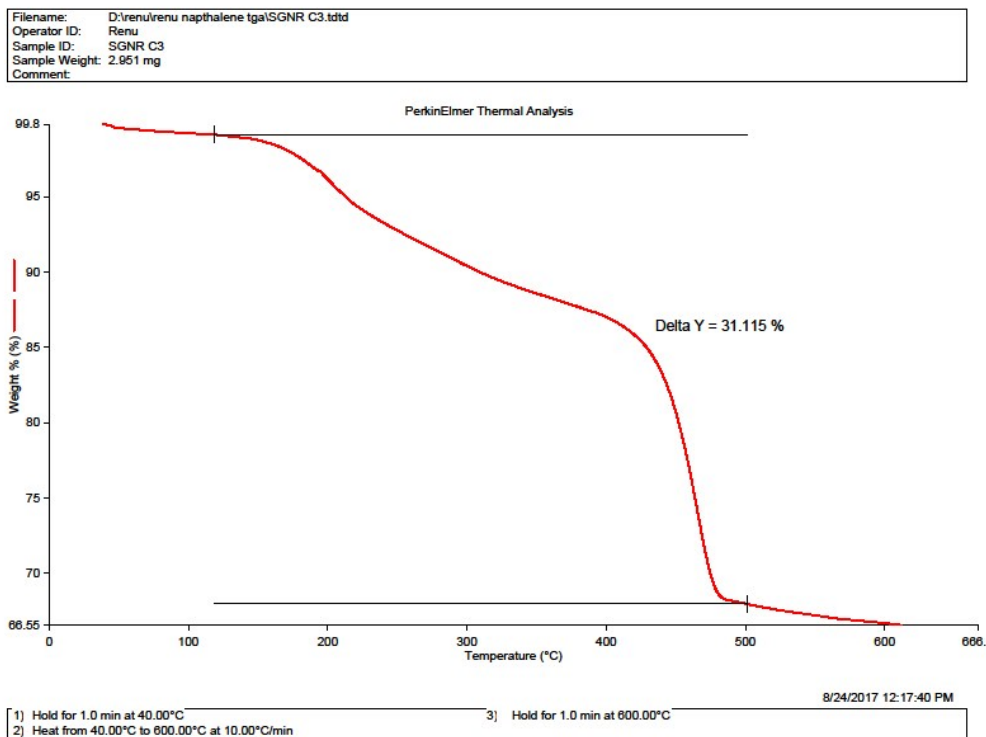


Fig. S76 TGA of NPs obtained from **3** after Sonogashira coupling reaction

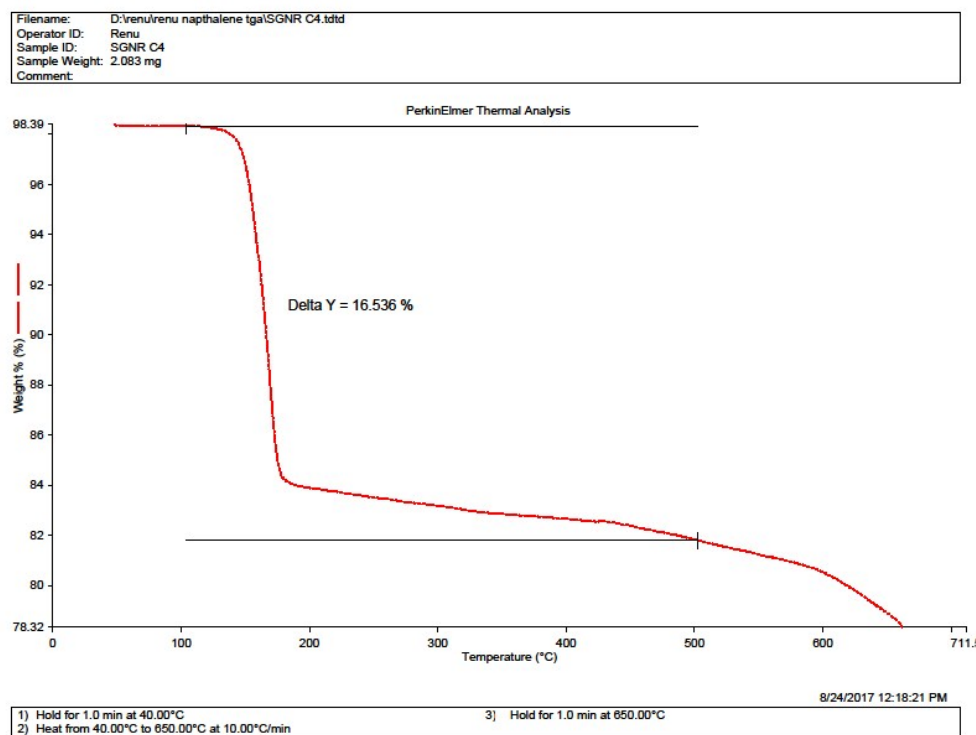


Fig. S77 TGA of NPs obtained from **4** after Sonogashira coupling reaction

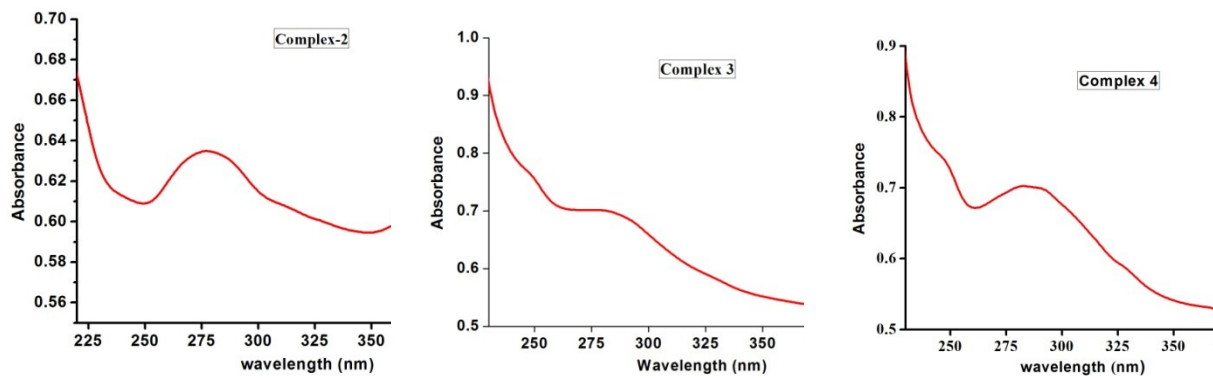


Fig. S78 UV-Vis spectrum of NPs isolated from **2-4** during SMC

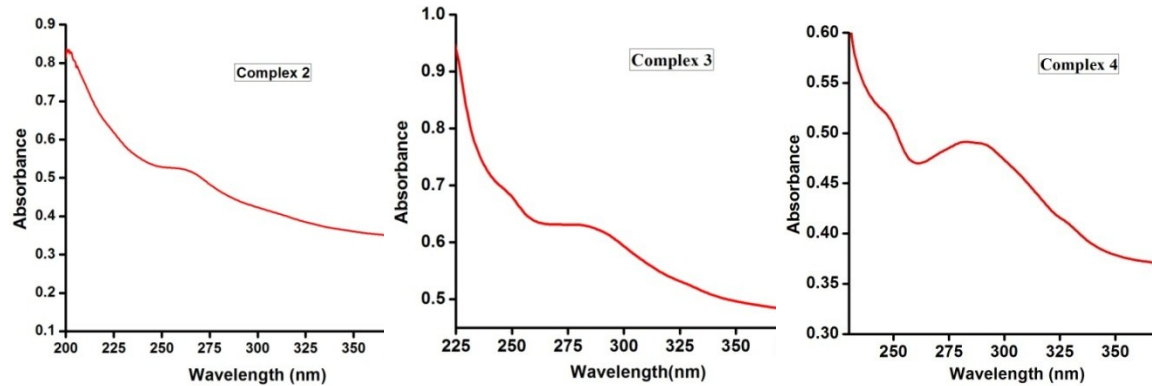


Fig. S79 UV-Vis spectrum of NPs isolated from **2-4** during Sonogashira coupling reaction

Agilent Resolutions Pro

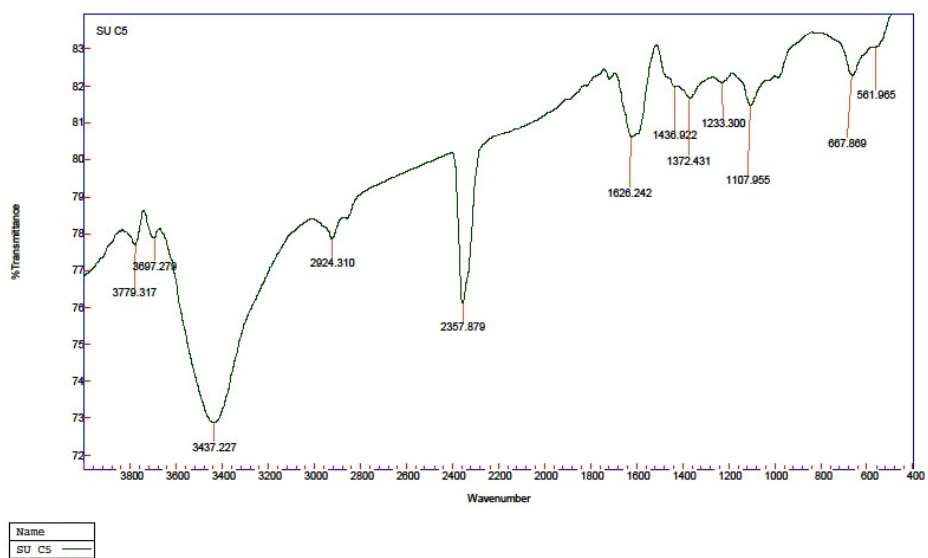


Fig. S80 FT-IR of NPs isolated from **1** during Sonogashira Coupling

Agilent Resolutions Pro

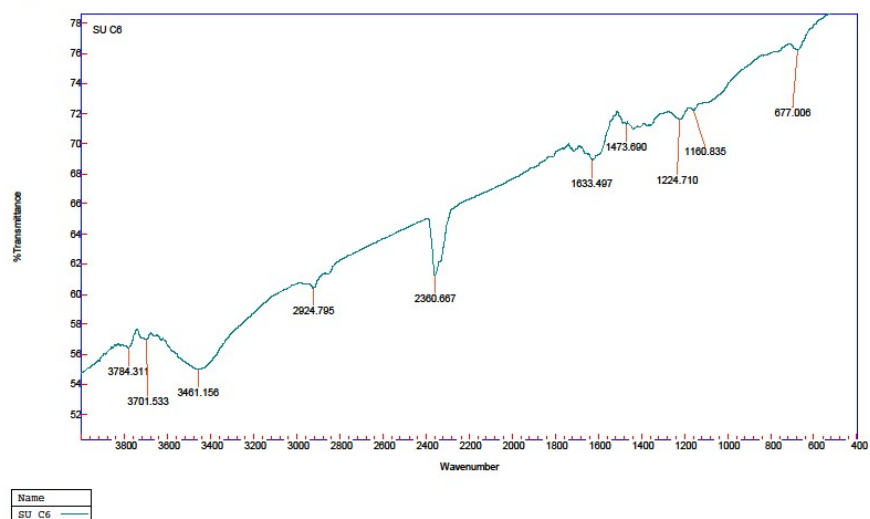


Fig. S81 FT-IR of NPs isolated from **2** during Sonogashira Coupling

Agilent Resolutions Pro

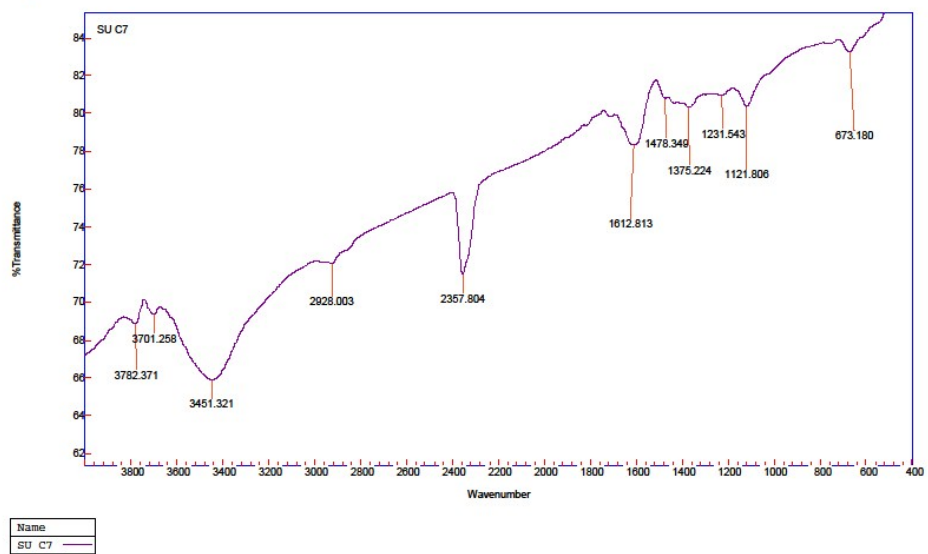


Fig. S82 FT-IR of NPs isolated from **3** during Sonogashira Coupling

Agilent Resolutions Pro

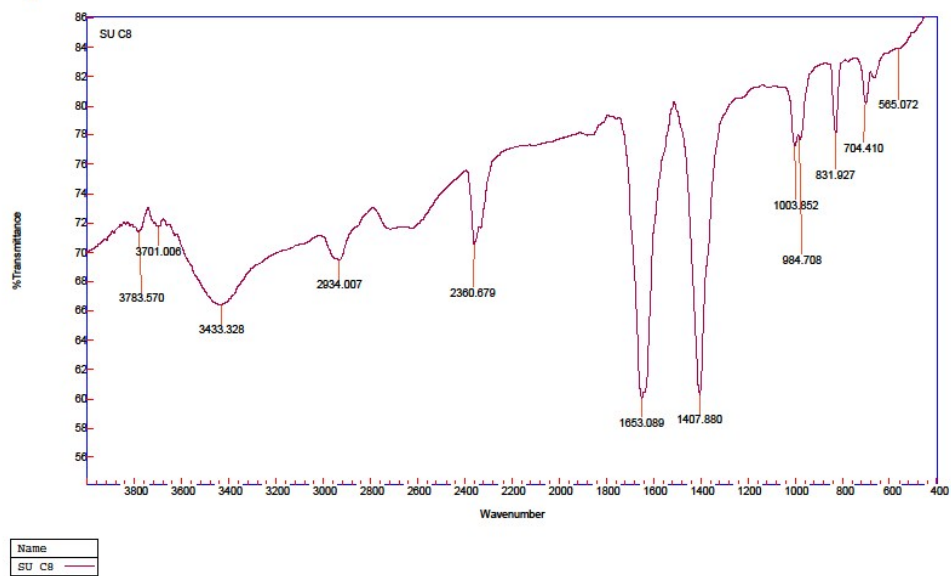


Fig. S83 FT-IR of NPs isolated from **4** during Sonogashira Coupling

Agilent Resolutions Pro

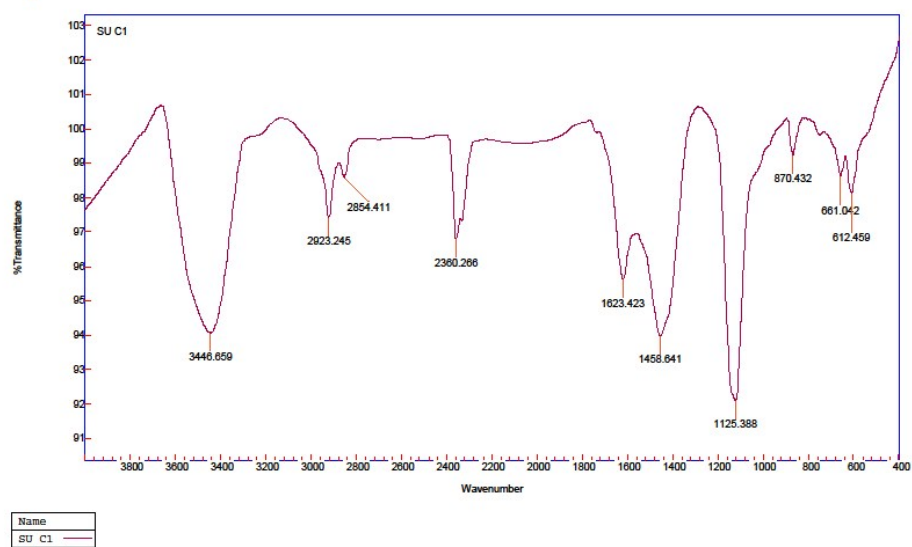


Fig. S84 FT-IR of NPs isolated from **1** during SMC

Agilent Resolutions Pro

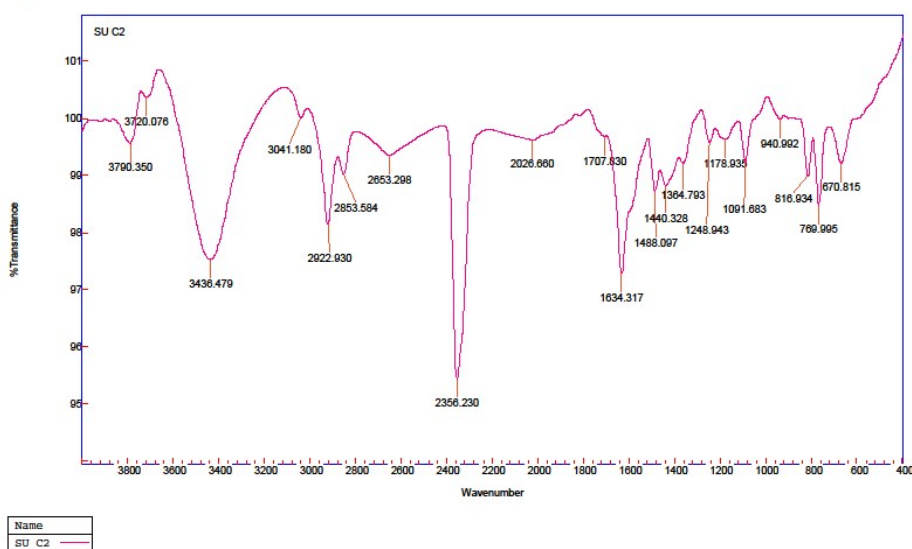


Fig. S85 FT-IR of NPs isolated from **2** during SMC

Agilent Resolutions Pro

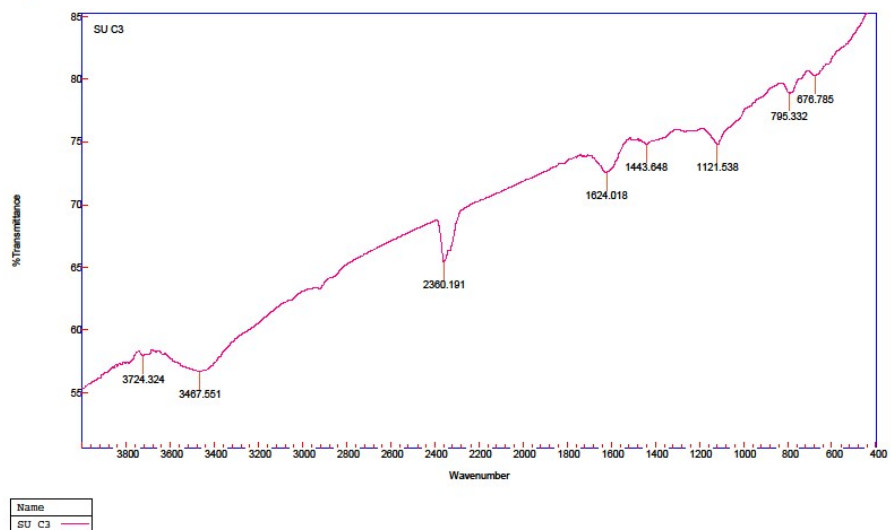


Fig. S86 FT-IR of NPs isolated from **3** during SMC

Agilent Resolutions Pro

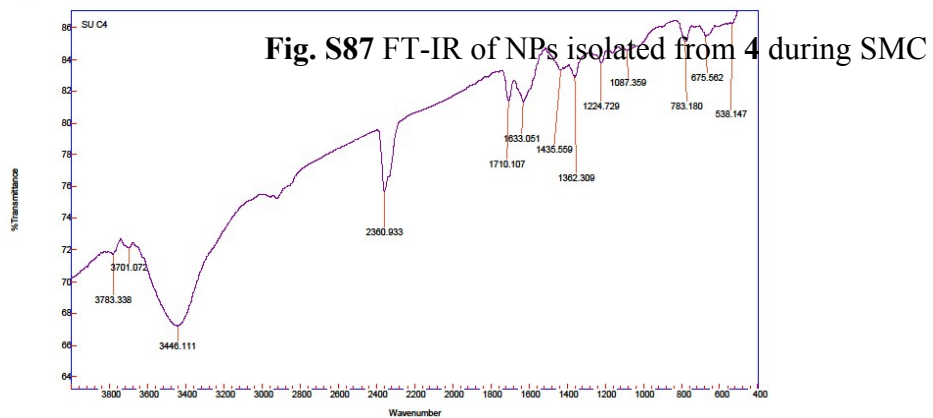


Fig. S87 FT-IR of NPs isolated from **4** during SMC

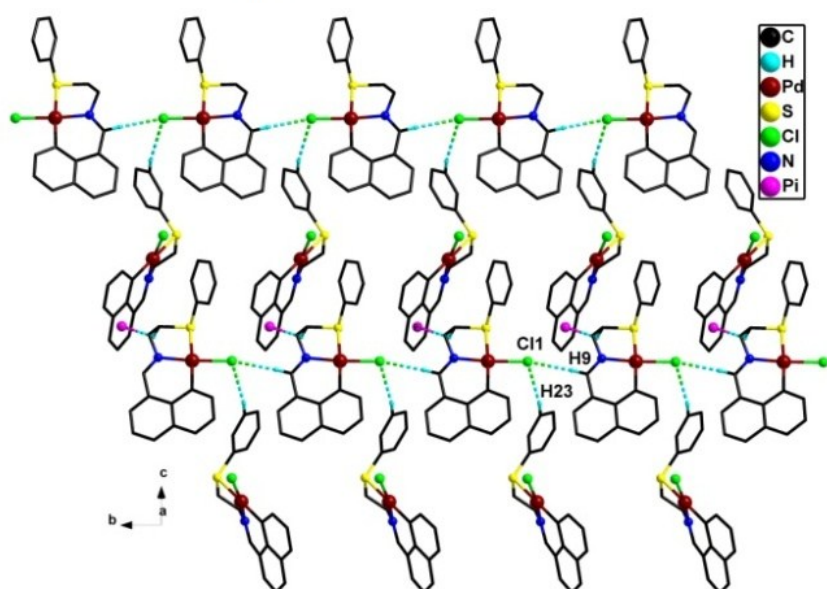


Fig. 88 Intermolecular C–H···Cl and C–H···π interaction in **1**; C–H9···Cl (2.690 Å), C–H23···Cl (2.711 Å) and C–H···π (3.037 Å)

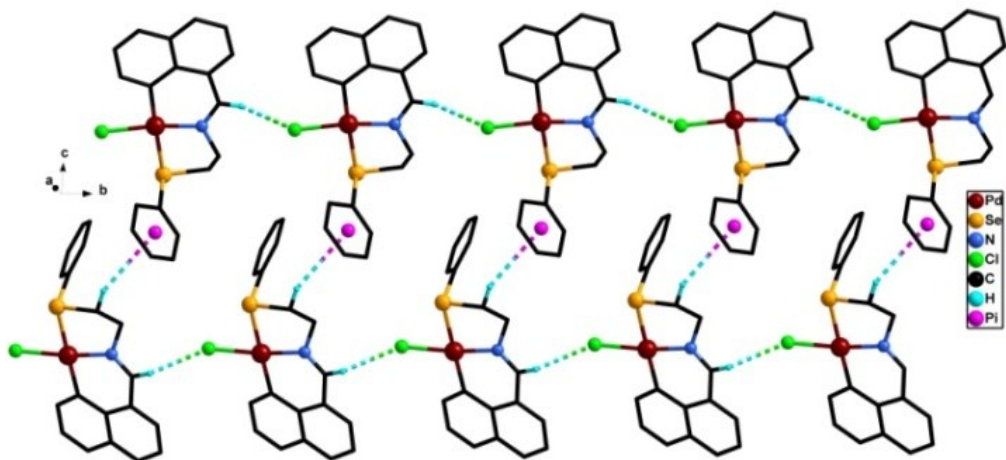


Fig. 89 Intermolecular interaction in **2**; C–H···Cl (2.711 Å) and C–H···π (2.832 Å)

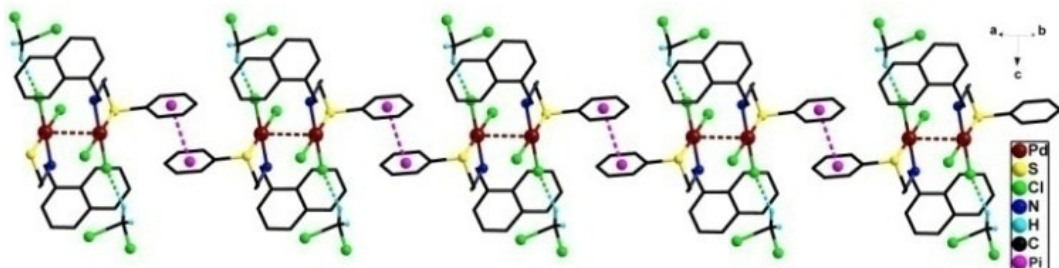


Fig. 90 Intermolecular interaction in **3**; C–H···Cl (2.644 Å) Pd···Pd (3.517 Å) and π···π (3.625 Å)

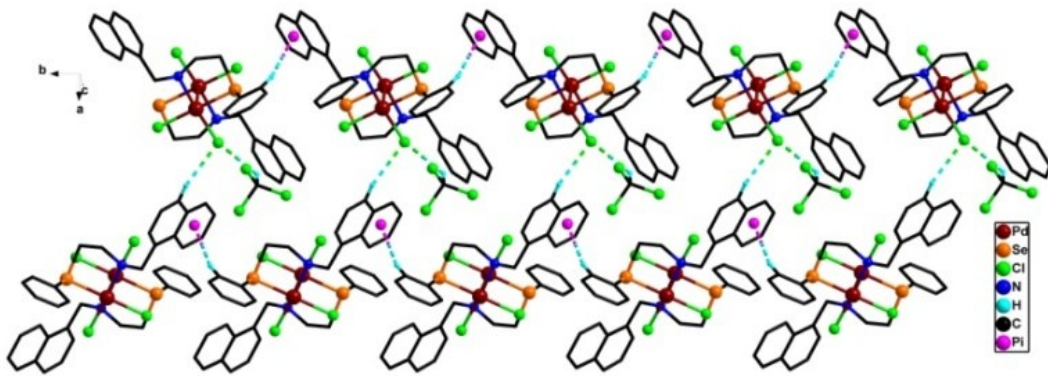


Fig. 91 Intermolecular interaction in **4**; C–H…Cl 2.859 Å and C–H…π (3.048 Å)

References

1. J. D. Webb, S. MacQuarrie, K. McEleney and C. M. Crudden, *J. Catal.*, 2007, **252**, 97–109.
2. R. N. Prabhu, S. Pal, *Tetrahedron Lett.*, 2015, **56**, 5252–5256.
3. F. Yang, X. Cui, Y. Li, J. Zhang, G. Ren and Y. Wu, *Tetrahedron*, 2007, **63**, 1963–1969.
4. Y. -B. Zhou, Y. -Q. Wang, L. -C. Ning, Z.-C. Ding, W.-L. Wang, C. -K. Ding, R. -H. Li, J. -J. Chen, X. Lu, Y. -J. Ding and Z. -P. Zhan, *J. Am. Chem. Soc.*, 2017, **139**, 3966–3969.
5. M. Gholinejad, J. Ahmadi, C. Najera, M. Seyedhamzeh, F. Zareh, M. K. –Zareh, *ChemCatChem*, 2017, **9**, 1442–1449.
6. A. K. Sharma, H. Joshi, R. Bhaskar, S. Kumar and A. K. Singh, *Dalton Trans.*, 2017, **46**, 2485–2496.

